



THE UNIVERSITY *of* EDINBURGH

Edinburgh Research Explorer

## Activity-Dependent Exocytosis of Lysosomes Regulates the Structural Plasticity of Dendritic Spines

**Citation for published version:**

Padamsey, Z, McGuinness, L, Bardo, SJ, Reinhart, M, Tong, R, Hedegaard, A, Hart, ML & Emptage, NJ 2017, 'Activity-Dependent Exocytosis of Lysosomes Regulates the Structural Plasticity of Dendritic Spines', *Neuron*, vol. 93, no. 1, pp. 132-146. <https://doi.org/10.1016/j.neuron.2016.11.013>

**Digital Object Identifier (DOI):**

[10.1016/j.neuron.2016.11.013](https://doi.org/10.1016/j.neuron.2016.11.013)

**Link:**

[Link to publication record in Edinburgh Research Explorer](#)

**Document Version:**

Publisher's PDF, also known as Version of record

**Published In:**

Neuron

**Publisher Rights Statement:**

Neuron 93, 132–146, January 4, 2017 Crown Copyright © 2017 Published by Elsevier Inc. This is an open access article under the CC BY license (<http://creativecommons.org/licenses/by/4.0/>).

**General rights**

Copyright for the publications made accessible via the Edinburgh Research Explorer is retained by the author(s) and / or other copyright owners and it is a condition of accessing these publications that users recognise and abide by the legal requirements associated with these rights.

**Take down policy**

The University of Edinburgh has made every reasonable effort to ensure that Edinburgh Research Explorer content complies with UK legislation. If you believe that the public display of this file breaches copyright please contact [openaccess@ed.ac.uk](mailto:openaccess@ed.ac.uk) providing details, and we will remove access to the work immediately and investigate your claim.



# Activity-Dependent Exocytosis of Lysosomes Regulates the Structural Plasticity of Dendritic Spines

## Highlights

- Back-propagating action potentials induce  $\text{Ca}^{2+}$  release from lysosomes in neurons
- Lysosomal  $\text{Ca}^{2+}$  release triggers exocytosis of the lysosomal protease Cathepsin B
- Cathepsin B maintains activity-dependent dendritic spine growth by activating MMP-9

## Authors

Zahid Padamsey,  
Lindsay McGuinness,  
Scott J. Bardo, ..., Anne Hedegaard,  
Michael L. Hart, Nigel J. Emptage

## Correspondence

nigel.emptage@pharm.ox.ac.uk

## In Brief

Padamsey et al. find that back-propagating action potentials trigger  $\text{Ca}^{2+}$  release from lysosomes in hippocampal pyramidal dendrites. This  $\text{Ca}^{2+}$  release results in the exocytosis of the lysosomal protease Cathepsin B, which activates MMP-9 to maintain activity-dependent spine growth.



# Activity-Dependent Exocytosis of Lysosomes Regulates the Structural Plasticity of Dendritic Spines

Zahid Padamsey,<sup>1</sup> Lindsay McGuinness,<sup>1</sup> Scott J. Bardo,<sup>1</sup> Marcia Reinhart,<sup>1</sup> Rudi Tong,<sup>1</sup> Anne Hedegaard,<sup>1</sup> Michael L. Hart,<sup>1</sup> and Nigel J. Emptage<sup>1,2,\*</sup>

<sup>1</sup>Department of Pharmacology, University of Oxford, Mansfield Road, Oxford, OX1 3QT, UK

<sup>2</sup>Lead Contact

\*Correspondence: [nigel.emptage@pharm.ox.ac.uk](mailto:nigel.emptage@pharm.ox.ac.uk)

<http://dx.doi.org/10.1016/j.neuron.2016.11.013>

## SUMMARY

Lysosomes have traditionally been viewed as degradative organelles, although a growing body of evidence suggests that they can function as  $\text{Ca}^{2+}$  stores. Here we examined the function of these stores in hippocampal pyramidal neurons. We found that back-propagating action potentials (bpAPs) could elicit  $\text{Ca}^{2+}$  release from lysosomes in the dendrites. This  $\text{Ca}^{2+}$  release triggered the fusion of lysosomes with the plasma membrane, resulting in the release of Cathepsin B. Cathepsin B increased the activity of matrix metalloproteinase 9 (MMP-9), an enzyme involved in extracellular matrix (ECM) remodelling and synaptic plasticity. Inhibition of either lysosomal  $\text{Ca}^{2+}$  signaling or Cathepsin B release prevented the maintenance of dendritic spine growth induced by Hebbian activity. This impairment could be rescued by exogenous application of active MMP-9. Our findings suggest that activity-dependent exocytosis of Cathepsin B from lysosomes regulates the long-term structural plasticity of dendritic spines by triggering MMP-9 activation and ECM remodelling.

## INTRODUCTION

Lysosomes are classically viewed as degradative organelles (Luzio et al., 2007b). Several studies, however, have demonstrated that lysosomes, along with other related acidic organelles, comprise additional sources of intracellular  $\text{Ca}^{2+}$ . Notably, these sources are distinct from the endoplasmic reticulum (ER) and mitochondria (Galione, 2015). In this paper, we use the term lysosome to collectively refer to the lysosome and its related acidic organelles.

$\text{Ca}^{2+}$  signaling from lysosomes has now been described in a number of cell types (Galione et al., 2010, 2015).  $\text{Ca}^{2+}$  storage in the lysosome requires an  $\text{H}^{+}$  gradient, which is generated by a vacuolar  $\text{H}^{+}$ -ATPase (V-ATPase), and some form of  $\text{Ca}^{2+}/\text{H}^{+}$  exchange (Morgan et al., 2011).  $\text{Ca}^{2+}$  release from the lysosomes requires the second messenger nicotinic acid adenine dinucleo-

tide phosphate (NAADP), which is synthesized, most likely by ADP-ribosyl cyclases, in response to cell-specific physiological stimuli (Galione et al., 2010, 2015). NAADP-dependent  $\text{Ca}^{2+}$  efflux from lysosomes is thought to occur either via transient receptor potential cation channels of the mucolipin 1 family (TRPML1) or via two-pore channels (TPC1/TPC2) (Guse, 2012), with the weight of evidence currently suggesting that NAADP acts via TPCs, most likely via an NAADP-associated binding protein (Morgan and Galione, 2014; Morgan et al., 2015b).

NAADP-dependent lysosomal  $\text{Ca}^{2+}$  signaling is likely to play a role in neurons. NAADP binding sites have been found throughout the brain (Patel et al., 2000), and NAADP synthesis and lysosomal  $\text{Ca}^{2+}$  release in neurons can be triggered by exogenous stimulation with glutamate (Pandey et al., 2009). Moreover, application of NAADP elicits  $\text{Ca}^{2+}$  release in brain microsomes (Bak et al., 1999), promotes neuronal differentiation in PC12 cells (Brailoiu et al., 2006), augments neurite outgrowth in developing cortical neurons (Brailoiu et al., 2005), drives membrane depolarization in medullary neurons (Brailoiu et al., 2009), and increases  $\text{Ca}^{2+}$  influx through N-type voltage-gated  $\text{Ca}^{2+}$  channels (VGCCs) in cultured hippocampal neurons (Hui et al., 2015). Lysosomes have also been found in axonal boutons, and pharmacologically induced  $\text{Ca}^{2+}$  release from these organelles can drive spontaneous neurotransmitter release (Brailoiu et al., 2003; McGuinness et al., 2007). Lysosomal  $\text{Ca}^{2+}$  release, however, has not been investigated in postsynaptic structures or in the context of synaptic plasticity.

In addition to mediating  $\text{Ca}^{2+}$  signaling, the lysosome itself can also undergo  $\text{Ca}^{2+}$ -dependent fusion, both with other organelles and with the plasma membrane (Luzio et al., 2007b). In the latter case, lysosomal exocytosis can be important in some cell types for the secretion of chemical signals or enzymes (Blott and Griffiths, 2002; Zhang et al., 2007; Galione et al., 2010; Davis et al., 2012; Galione, 2015) or for promoting lipid turnover and facilitating membrane growth and repair (Reddy et al., 2001; Blott and Griffiths, 2002; Luzio et al., 2007b). Although not well studied, lysosomal fusion has been reported in developing hippocampal and sympathetic neuronal cultures, where it regulates the surface expression of N-type VGCCs and the outgrowth of neurites, respectively (Arantes and Andrews, 2006; Hui et al., 2015). However, it is not clear what physiological trigger drives lysosomes to fuse with the plasma membrane or the significance of this fusion for information processing in neurons.

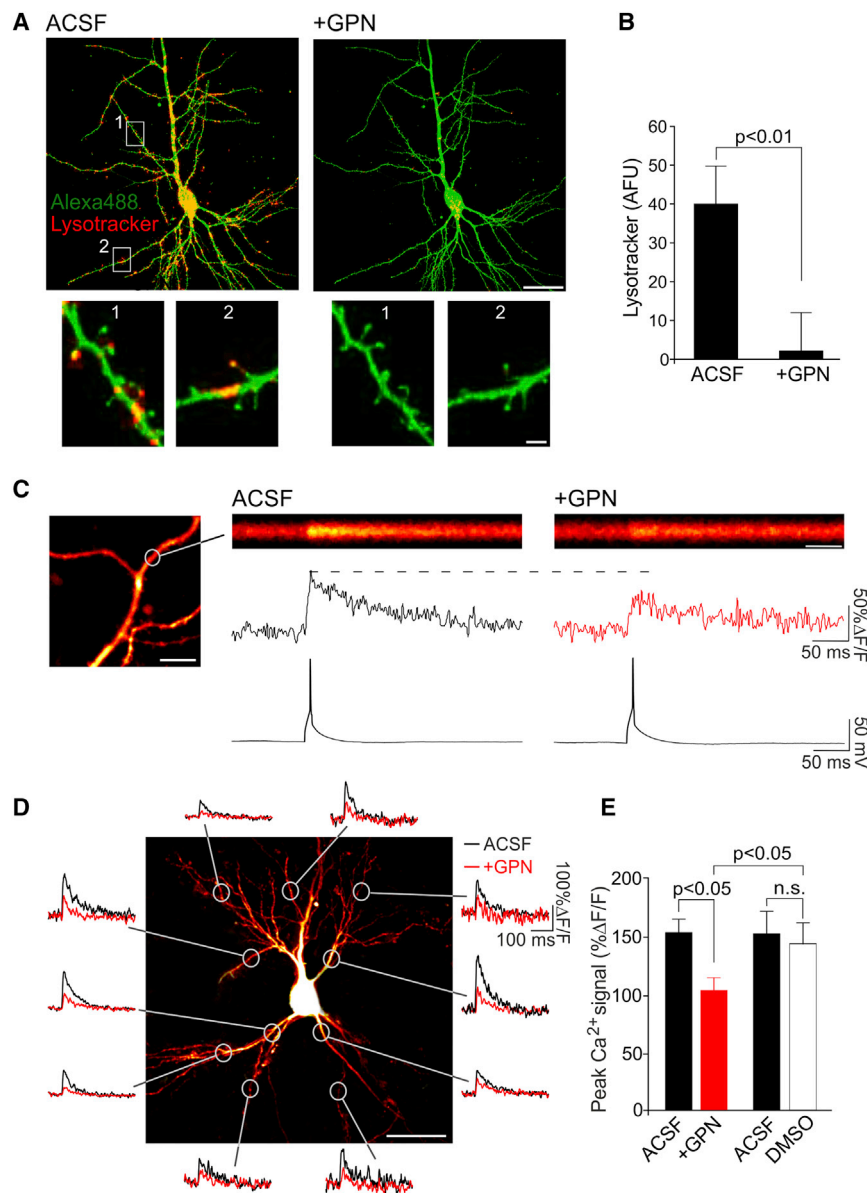


**Figure 1. Lysosomes Contribute to bpAP-Evoked Dendritic Ca<sup>2+</sup> Signaling**

(A) Top: CA1 neuron loaded with Alexa 488 (green) and stained with LysoTracker (red) (scale bar, 10  $\mu$ m). Disruption of the lysosomal membrane with GPN abolished LysoTracker staining. Regions of interest (white boxes) are magnified below (scale bar, 2  $\mu$ m).

(B) Average LysoTracker staining in ACSF (artificial cerebrospinal fluid) and GPN ( $n = 5$  cells/condition). Significance was assessed with a Mann-Whitney test.

(C) Example bpAP-evoked Ca<sup>2+</sup> transient in CA1 apical dendrites loaded with OGB-1 (scale bar, 10  $\mu$ m). Laser scanning was restricted to a line across a region of interest (circle). The resulting line scan (scale bar, 50 ms), along with its quantification (%ΔF/F) is shown time-locked with electrophysiological recordings. GPN reduced the bpAP-evoked Ca<sup>2+</sup> influx.

(D) CA1 neuron loaded with OGB-1. Ca<sup>2+</sup> transients evoked before (black traces) and after (red traces) the addition of GPN are shown for regions of interest (scale bar, 20  $\mu$ m).

(E) Average data ( $n = 7$ –18 cells/condition). Significance was assessed with Kruskal-Wallis and post hoc Dunn's tests. Error bars represent SEM. See also Figures S1 and S2.

Here we examined the role of lysosomes in hippocampal pyramidal neurons. We found that lysosomal Ca<sup>2+</sup> signaling and lysosomal fusion with the plasma membrane were driven by back-propagating action potentials (bpAPs) and were necessary for the long-term structural plasticity of dendritic spines.

## RESULTS

### Lysosomes Contribute to bpAP-Evoked Dendritic Ca<sup>2+</sup> Signaling

We began by examining the distribution of lysosomes in hippocampal pyramidal neurons. To do so, we incubated hippocampal slice cultures with LysoTracker red (50 nM, 40–60 min), a fluorescent dye that preferentially labels lysosomal compartments (Chazotte, 2011). We found LysoTracker-labeled puncta

throughout the dendritic arbor of CA3 and CA1 neurons and in some dendritic spines (Figure 1A). To confirm that LysoTracker fluorescence was specific for lysosomes, we used glycyl-L-phenylalanine 2-naphthylamide (GPN, 200  $\mu$ M, 5–10 min) to selectively disrupt lysosomal compartments. GPN is a cell-permeable substrate for the lysosome-specific enzyme Cathepsin C. When cleaved, GPN becomes membrane-impermeable and exerts an osmotic effect that disrupts the lysosomal membrane, leading to the leakage of small molecules out of the organelle (Penny et al., 2014). We found that addition of GPN abolished the vast

majority of LysoTracker fluorescence in cells ( $n = 5$  cells; Mann-Whitney test,  $p < 0.01$ ; Figure 1B), suggesting that LysoTracker was predominantly labeling lysosomal compartments. Notably, GPN-induced disruption of the lysosomal membrane was not accompanied by any detrimental effects on neuronal morphology (Figure 1A), resting membrane potential, conductance, and intracellular pH (Figures S1 and S2).

We next examined whether lysosomes contributed to dendritic Ca<sup>2+</sup> signaling during neuronal activity. We loaded CA3 and CA1 neurons with the Ca<sup>2+</sup>-sensitive dye Oregon Green BAPTA-1 (OGB-1) and imaged dendritic Ca<sup>2+</sup> in response to single bpAPs (Figure 1C). bpAP-evoked Ca<sup>2+</sup> influx is thought to be predominantly, if not exclusively, mediated by VGCCs (Jaffe et al., 1992; Christie et al., 1995; Spruston et al., 1995; Helmchen et al., 1996). However, we found that GPN, despite

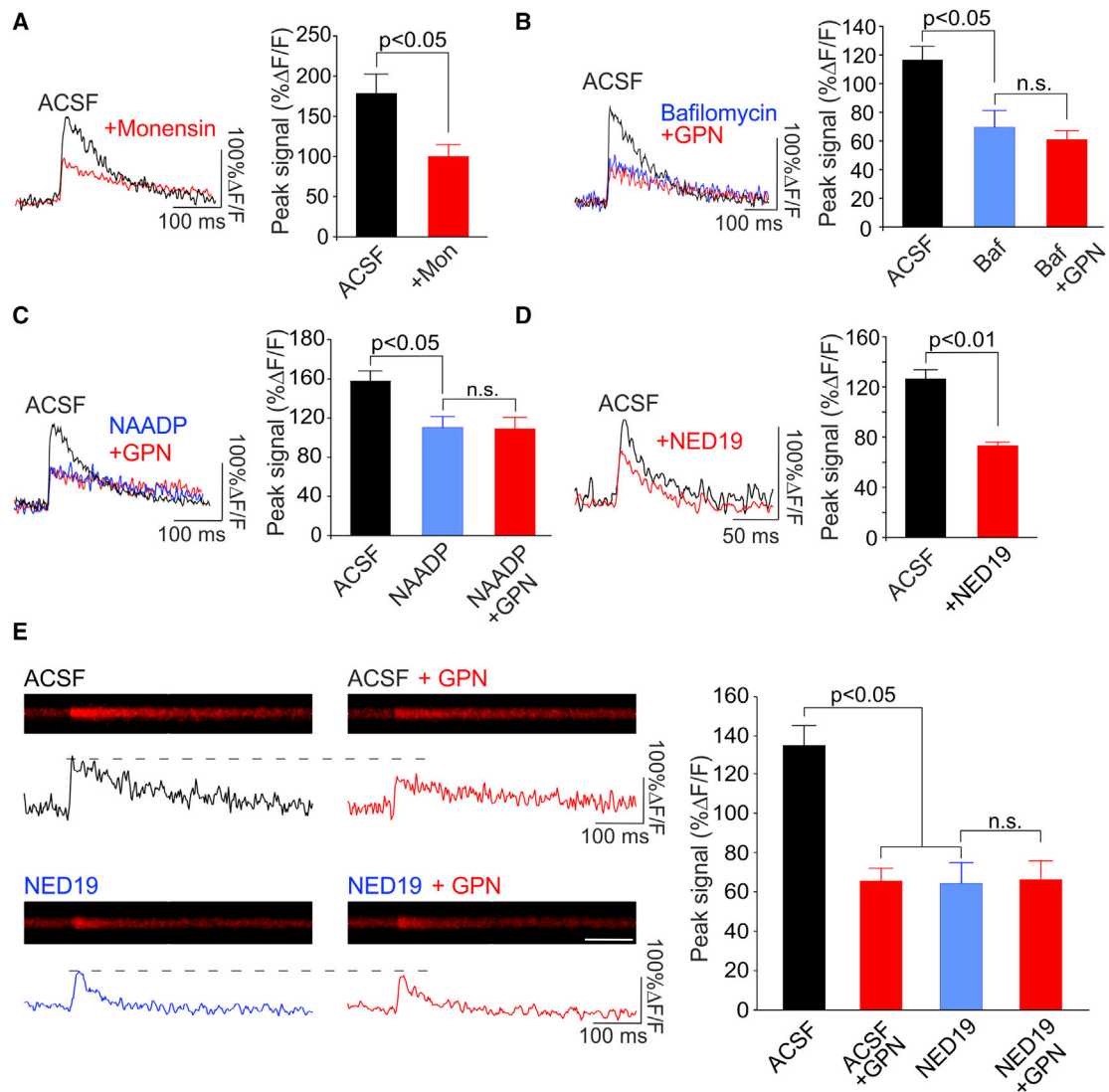


**Figure 2. Lysosomal  $\text{Ca}^{2+}$  Release Requires NAADP**

(A–D) Left: sample  $\text{Ca}^{2+}$  transients evoked by single bpAPs in CA1 apical dendrites.  $\text{Ca}^{2+}$  transients were reduced following inhibition of lysosomal  $\text{Ca}^{2+}$  signaling by various reagents. Right: average peak  $\text{Ca}^{2+}$  signal measured across conditions ( $n = 5$ –10 cells/condition). Significance was assessed with Mann-Whitney tests (single comparisons) or Kruskal-Wallis and post hoc Dunn's tests (multiple comparisons).

(E) Left: example of line scan images (scale bar, 100 ms) and quantified traces (%ΔF/F) of  $\text{Ca}^{2+}$  signals recorded in CA1 apical dendrites in acute hippocampal slices. Right: average peak fluorescence ( $n = 6$ –7 cells/condition).  $\text{Ca}^{2+}$  transients were reduced by GPN and NED-19. Significance was assessed with Kruskal-Wallis and post hoc Dunn's tests.

Error bars represent SEM. See also Figures S1–S5.

having no effect on the action potential waveform (Figure S1), significantly reduced the  $\text{Ca}^{2+}$  rise evoked by a single bpAP (in %ΔF/F; artificial cerebrospinal fluid [ACSF],  $153 \pm 11$ ; GPN,  $103 \pm 10$ ;  $n = 18$  cells; post hoc Dunn's test,  $p < 0.01$ ; Figures 1C–1E); these reductions were found throughout the dendritic arbor (Figure 1D) and were also present in acute hippocampal slices ( $n = 6$  cells; post hoc Dunn's test,  $p < 0.05$ ; Figures 2E and 2F). In contrast, application of vehicle control (DMSO) alone had no effect on bpAP-evoked  $\text{Ca}^{2+}$  transients ( $n = 7$  cells; post hoc Dunn's test,  $p = 0.99$ ; Figure 1E).

### Lysosomal $\text{Ca}^{2+}$ Release Requires NAADP

To confirm that neuronal activity could trigger  $\text{Ca}^{2+}$  release from the lysosomes, we used additional means of pharmacologically impairing lysosomal  $\text{Ca}^{2+}$  signaling (Galione, 2015; Morgan et al., 2015a; Figure 8B). We started by specifically inhibiting lysosomal  $\text{Ca}^{2+}$  storage, which requires a proton gradient to be established by V-ATPases (Morgan et al., 2011). To disrupt this gradient, we bath-applied the membrane-permeable  $\text{Na}^+/\text{H}^+$  ionophore monensin (20  $\mu\text{M}$ , 5–10 min). Monensin reduced the bpAP-evoked  $\text{Ca}^{2+}$  transient (in %ΔF/F; ACSF,  $179 \pm 24$ ; monensin,  $100 \pm 14$ ;  $n = 6$  cells; Mann-Whitney test,  $p < 0.05$ ; Figure 2A)



despite having no effect on action potential waveform (Figure S1). However, as previously reported, application of monensin resulted in membrane hyperpolarization (Figure S1), likely related to a modest alkalization of intracellular pH (Figure S2; Erecińska et al., 1991). Therefore, we conducted additional experiments in which lysosomal  $\text{Ca}^{2+}$  storage was disrupted using the V-ATPase inhibitor bafilomycin. Given the poor membrane permeability of the drug, we pre-incubated slices with bafilomycin (4  $\mu\text{M}$ , 1–2 hr). This had no effect on the action potential waveform or on the resting membrane potential (Figure S1) but caused a significant decrease in the bpAP-associated  $\text{Ca}^{2+}$  signal that was comparable in magnitude to the decrease obtained in monensin ( $n = 6$  cells/condition; bafilomycin versus control; post hoc Dunn's test,  $p < 0.05$ ; Figure 2B). Notably, subsequent addition of GPN resulted in no further reduction in the  $\text{Ca}^{2+}$  signal ( $n = 6$  cells; bafilomycin versus GPN, post hoc Dunn's test,  $p = 0.99$ ; Figure 2B), suggesting that the effects of bafilomycin were due to its inhibition of the proton gradient in lysosomes as opposed to other organelles.

We next inhibited lysosomal  $\text{Ca}^{2+}$  release. Lysosomal  $\text{Ca}^{2+}$  release requires NAADP, which most likely acts on TPCs (Morgan et al., 2015b). Although low concentrations of NAADP (10–100 nM) evoke  $\text{Ca}^{2+}$  efflux from the lysosome, higher concentrations (>100  $\mu\text{M}$ ) inhibit it via desensitization of the  $\text{Ca}^{2+}$  release machinery (Berg et al., 2000; Masgrau et al., 2003). Consistent with this, we found that a concentration of 1 mM NAADP in the patch electrode could inhibit lysosomal  $\text{Ca}^{2+}$  release in hippocampal neurons (Figure S3). We also found that this concentration of NAADP reduced the bpAP-evoked  $\text{Ca}^{2+}$  signal (in  $\% \Delta F/F$ ; ACSF,  $158 \pm 10$ ; NAADP desensitization,  $110 \pm 11$ ;  $n = 5$  cells; post hoc Dunn's test,  $p < 0.05$ ; Figure 2C) and occluded the effects of GPN ( $n = 5$  cells; NAADP versus GPN, post hoc Dunn's test,  $p = 0.94$ ; Figure 2C). Similar reductions in  $\text{Ca}^{2+}$  influx were also observed with the cell-permeable NAADP antagonist NED-19 (100  $\mu\text{M}$ , 30-to 60-min pre-incubation;  $n = 10$  cells; Mann-Whitney test,  $p < 0.01$ ; Figure 2D). NED-19 also decreased the bpAP-associated  $\text{Ca}^{2+}$  signal in acute hippocampal slices ( $n = 6$  cells; post hoc Dunn's test,  $p < 0.05$ ; Figure 2E), and, again, such reductions occluded the effects of GPN ( $n = 6$  cells; NED-19 versus GPN, post hoc Dunn's test,  $p = 0.48$ ; Figure 2E).

Notably, drug-induced decreases in bpAP-evoked  $\text{Ca}^{2+}$  release did not result from direct inhibition of VGCC currents (Figure S4) or by affecting  $\text{Ca}^{2+}$  handling (Figure S5) but were likely due to inhibition of lysosomal  $\text{Ca}^{2+}$  signaling itself.

### **$\text{Ca}^{2+}$ Influx through VGCCs Triggers Lysosomal $\text{Ca}^{2+}$ Release**

Although NAADP is a necessary trigger for lysosomal  $\text{Ca}^{2+}$  release, it alone does not explain how an electrical signal, such as a bpAP, triggers  $\text{Ca}^{2+}$  release from the lysosome. We hypothesized that an additional voltage-sensitive mechanism that gates or modulates lysosomal  $\text{Ca}^{2+}$  release must be present. One possibility is that the lysosomal  $\text{Ca}^{2+}$  release machinery may be directly voltage-sensitive (Rybalchenko et al., 2012; Cang et al., 2014; Pitt et al., 2014). Alternatively, lysosomes may sense voltage indirectly via functional coupling with plasma membrane voltage-gated channels. This coupling may be direct,

as in the case of the mechanical coupling between ryanodine receptors and VGCCs in striated muscle (Sandow, 1952). This coupling may also be indirect and mediated by a second messenger such as  $\text{Ca}^{2+}$ . Indeed, it is known that  $\text{Ca}^{2+}$  can trigger NAADP-dependent lysosomal  $\text{Ca}^{2+}$  release (Patel et al., 2001; Morgan et al., 2013), potentially by directly activating TPCs (Pitt et al., 2010, 2014). Thus, it is possible that  $\text{Ca}^{2+}$  influx from VGCCs during bpAPs may trigger  $\text{Ca}^{2+}$  release from lysosomes.

To distinguish between these possibilities, we first attempted to image lysosomal  $\text{Ca}^{2+}$  release in the presence of  $\text{Ni}^{2+}$  (100  $\mu\text{M}$ ) and  $\text{Cd}^{2+}$  (100  $\mu\text{M}$ ) to inhibit VGCCs. This would determine whether the lysosomes could release  $\text{Ca}^{2+}$  independent of VGCC activity. Under these conditions, we could not detect any  $\text{Ca}^{2+}$  transients, either in response to a single bpAP ( $n = 6$  cells; post hoc Dunn's test,  $p = 0.99$ ; Figures 3A and 3B) or to a more potent, 200-ms step depolarization to >20 mV ( $n = 6$  cells; post hoc Dunn's test,  $p = 0.99$ ; Figures 3A and 3B) compared with unstimulated controls ( $n = 6$ ). These findings suggest that membrane voltage alone cannot elicit lysosomal  $\text{Ca}^{2+}$  release and that lysosomal  $\text{Ca}^{2+}$  signaling requires VGCC activation. To examine specifically whether it was the direct mechanical opening of VGCCs or VGCC-mediated  $\text{Ca}^{2+}$  influx that was triggering lysosomal  $\text{Ca}^{2+}$  release, we repeated our experiments in 0  $\text{Ca}^{2+}$  ACSF, which prevents VGCC-mediated  $\text{Ca}^{2+}$  influx but, unlike bath application of  $\text{Ni}^{2+}$  and  $\text{Cd}^{2+}$ , does so without potential interference of the mechanical opening and closing of VGCCs. Again, under these conditions, we were unable to detect any bpAP-evoked dendritic  $\text{Ca}^{2+}$  transients, either in response to a single bpAP ( $n = 5$  cells; post hoc Dunn's test,  $p = 0.99$ ; Figure 3B) or to a step depolarization to >20 mV ( $n = 5$  cells; post hoc Dunn's test,  $p = 0.99$ ; Figure 3B) compared with unstimulated controls ( $n = 6$ ). As a positive control, to ensure that our experimental setup was sensitive enough to detect lysosomal  $\text{Ca}^{2+}$  transients if present, we included low, physiologically relevant concentrations of NAADP (10–100 nM) in our recording electrode to directly trigger  $\text{Ca}^{2+}$  release from the lysosomes (Calcraft et al., 2009; Figure S3). Under these conditions, we could reliably detect small and rapid  $\text{Ca}^{2+}$  transients throughout the dendritic arbor that could be abolished by the NAADP antagonist NED-19. Collectively, our findings suggest that  $\text{Ca}^{2+}$  influx through VGCCs triggers lysosomal  $\text{Ca}^{2+}$  release. In this way, lysosomal  $\text{Ca}^{2+}$  stores are indirectly coupled to VGCCs, enabling them to be mobilized by changes in membrane voltage that occur during bpAPs.

In many cell types, lysosomal  $\text{Ca}^{2+}$  release is functionally coupled to  $\text{Ca}^{2+}$  release from the ER as opposed to VGCCs (Patel et al., 2001; Galione et al., 2010; Morgan and Galione, 2014). Previous studies, however, have demonstrated that the ER does not contribute to bpAP-evoked  $\text{Ca}^{2+}$  transients (Markram et al., 1995; Emptage et al., 1999; Kovalchuk et al., 2000), arguing against lysosome-ER coupling in neuronal dendrites. In line with this, we found that blocking ER  $\text{Ca}^{2+}$  signaling with either ryanodine (20  $\mu\text{M}$ , 20 min) or thapsigargin (15  $\mu\text{M}$ , 20 min) had no effect on the amplitude of bpAP-evoked  $\text{Ca}^{2+}$  transients ( $n = 5$  cells/condition; Kruskal-Wallis test,  $p > 0.05$ ; Figures 3C and 3D). In a subset of experiments with thapsigargin, subsequent addition of GPN resulted in the expected reduction of

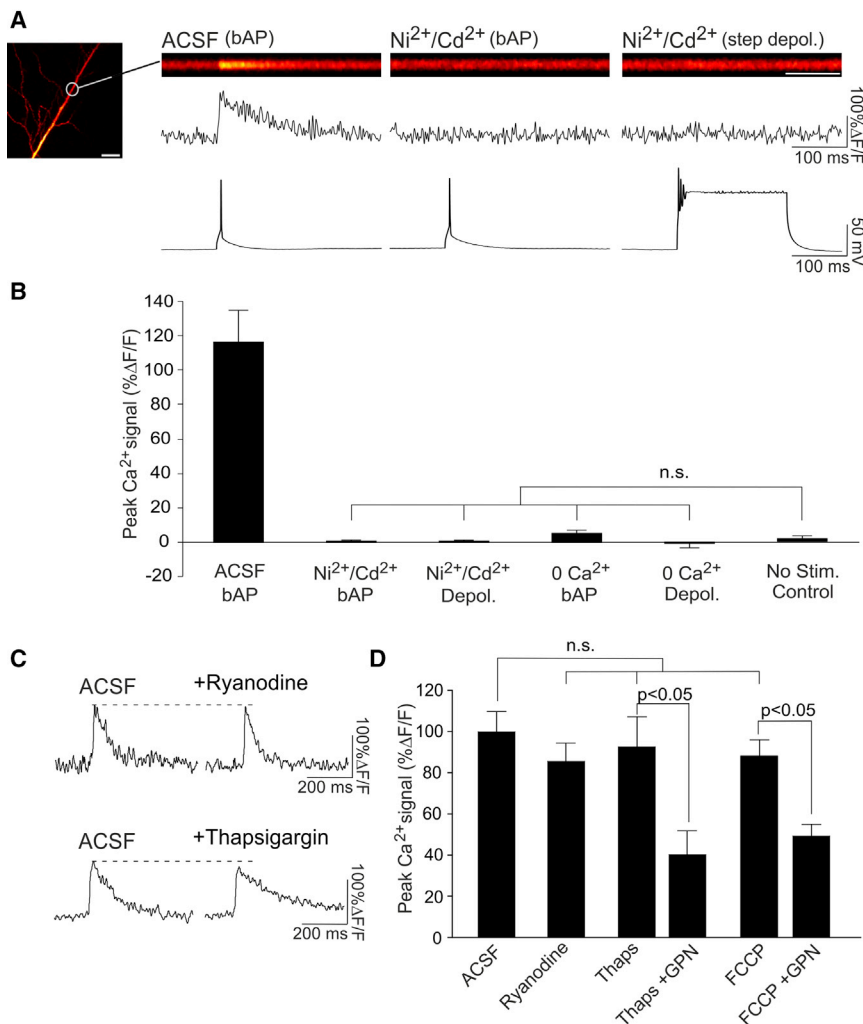


**Figure 3. Ca<sup>2+</sup> Influx through VGCCs Triggers Lysosomal Ca<sup>2+</sup> Release**

(A) Example line scan images (scale bar, 100 ms) and quantified traces (%ΔF/F) of bpAP-evoked Ca<sup>2+</sup> transients in CA1 apical dendrites (scale bar, 10 μm) time-locked to electrophysiological recordings. Ni<sup>2+</sup> and Cd<sup>2+</sup> abolished Ca<sup>2+</sup> influx evoked either by a single bpAP or a 200-ms step depolarization to >20 mV.

(B) Average data. Ca<sup>2+</sup> transients were abolished by inhibition of VGCC-mediated Ca<sup>2+</sup> influx by Ni<sup>2+</sup>/Cd<sup>2+</sup> or 0 Ca<sup>2+</sup> and did not significantly differ from transients recorded in the absence of stimulation (no stim. control) (n = 5–6 cells/condition).

(C) Sample bpAP-evoked Ca<sup>2+</sup> transients shown before and after the presence of ryanodine or thapsigargin to inhibit Ca<sup>2+</sup> signaling from the ER.

(D) Average peak Ca<sup>2+</sup> transients. Inhibition of ER or mitochondrial Ca<sup>2+</sup> signaling (FCCP) had no effect on bpAP-evoked Ca<sup>2+</sup> transients and failed to occlude the effects of GPN (n = 3–5 cells/condition). Significance was assessed with paired t tests (single paired comparisons) or Kruskal-Wallis and post hoc Dunn's tests (multiple comparisons). Error bars represent SEM. See also Figure S3.

bpAP-evoked Ca<sup>2+</sup> signaling (n = 3 cells; paired t test, p < 0.05; Figures 3C and 3D). Collectively, these findings suggest that the ER is unlikely to play a role in bpAP-evoked lysosomal Ca<sup>2+</sup> release.

We also examined the possibility that lysosomal Ca<sup>2+</sup> release was coupled to mitochondrial Ca<sup>2+</sup> stores. Consistent with a previous report (Markram et al., 1995), application of the mitochondrial uncoupler FCCP (1 μM, 5 min) had no effect on bpAP-evoked Ca<sup>2+</sup> transients (n = 5 cells; Kruskal-Wallis test, p > 0.05; Figure 3D) and failed to occlude the effects of GPN (n = 5 cells; paired t test, p < 0.05; Figure 3D). These findings suggest that, under our experimental conditions, the lysosome is the only internal Ca<sup>2+</sup> store that contributes to bpAP-evoked Ca<sup>2+</sup> signaling and is functionally coupled to VGCCs.

### Lysosomal Ca<sup>2+</sup> Signaling Drives Fusion of the Lysosomes with the Plasma Membrane

What might be the function of lysosomal Ca<sup>2+</sup> release in neurons? The lysosome itself is known to undergo Ca<sup>2+</sup>-dependent fusion both with other organelles and with the plasma membrane (Luzio et al., 2007b). The source of Ca<sup>2+</sup> in such instances can be

the lysosome itself (Pryor et al., 2000; Luzio et al., 2007a, 2007b; Davis et al., 2012; Galione, 2015). Lysosomal fusion to the plasma membrane has been shown to release chemical messengers or enzymes in several cell types (Luzio et al., 2007b; Galione, 2015). If present in neurons, such a mechanism could have implications for activity-dependent processing in dendrites. Additionally, our finding of the strong functional coupling between VGCC activation and lysosomal

Ca<sup>2+</sup> release in neurons suggests that lysosomes would be ideally situated for activity-dependent fusion with the plasma membrane, akin to synaptic vesicles in the presynaptic terminal.

We investigated whether activity-dependent release of Ca<sup>2+</sup> from the lysosome could trigger fusion of the lysosome to the plasma membrane in neuronal dendrites. We started by using total internal reflection fluorescence microscopy (TIRFM) to monitor the dynamics of LysoTracker-stained lysosomes near the plasma membrane in dissociated hippocampal cultures. We found weak LysoTracker labeling in the dendrites under baseline conditions (Figure 4A). However, when we elevated extracellular K<sup>+</sup> to 45 mM to drive strong dendritic depolarization and VGCC activity (Wu et al., 2001a, 2001b), we observed a marked increase in the intensity of labeled puncta (Figure 4B) and an overall increase in surface fluorescence (6.50%ΔF/F ± 0.05%ΔF/F; n = 5 cells; z test versus 0, p < 0.01; Figure 4A; Movie S1). Depolarization had no such effects on cells pre-incubated with NED-19, and, instead, only decreases in fluorescence were observed because of the effects of photobleaching (−1.62%ΔF/F ± 0.76%ΔF/F; n = 5 cells; NED-19 versus K<sup>+</sup>, Mann-Whitney test, p < 0.05; Figures 4A and 4B).

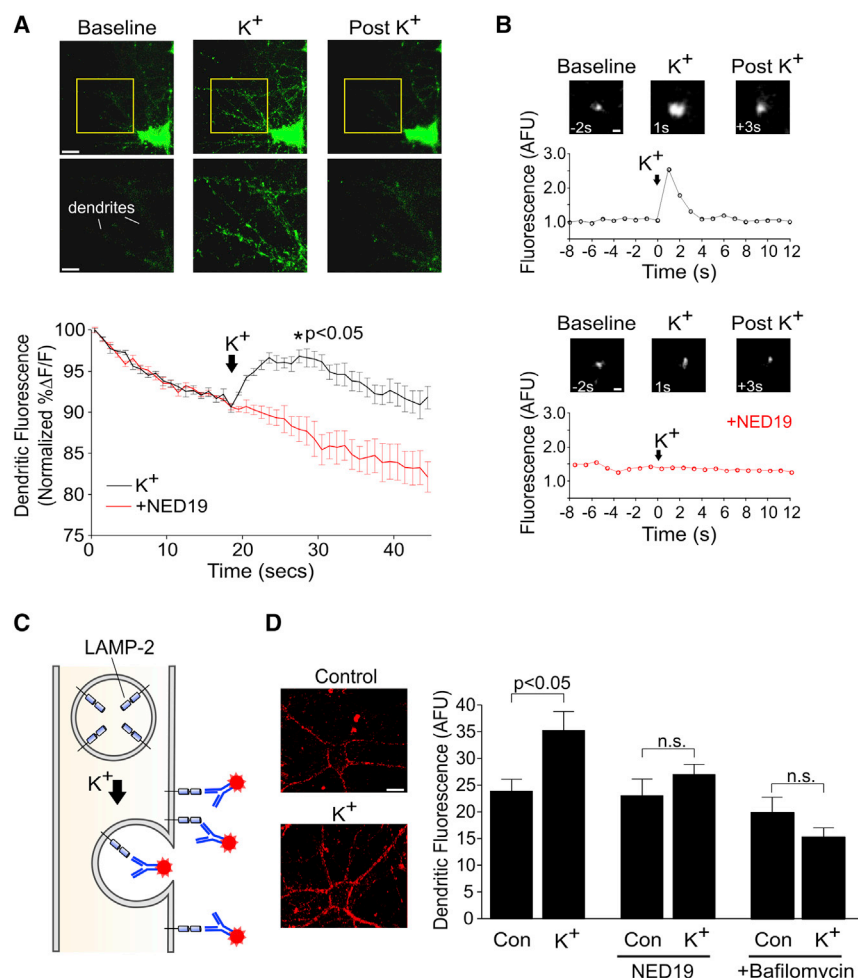


**Figure 4. Lysosomal  $Ca^{2+}$  Signaling Drives Fusion of the Lysosomes with the Plasma Membrane**

(A) Top: TIRFM images of a dissociated hippocampal neuron loaded with LysoTracker.  $K^+$  stimulation resulted in translocation of LysoTracker-stained puncta to the cell surface (scale bar, 10  $\mu m$ ). The imaged area in the yellow box is magnified below (scale bar, 5  $\mu m$ ). Bottom: average change in LysoTracker fluorescence across time ( $n = 5$  cells/condition).  $K^+$ -induced increases in fluorescence were abolished by NED-19. Time-dependent decreases in fluorescence reflected photobleaching. Significance was assessed with Mann-Whitney test at the peak of fluorescence.

(B) Sample TIRFM images of individual LysoTracker-stained puncta in (A) (scale bar, 2  $\mu m$ ). Graphs depict fluorescence intensity in AFU against time.

(C) Schematic of live-cell immunolabeling of LAMP-2. Fluorescently tagged antibodies targeting the luminal domain of LAMP-2 were applied to neuronal cultures during  $K^+$  stimulation. Fluorescent labeling would require fusion of the lysosome with the plasma membrane.

(D) Left: sample images depicting surface LAMP-2 antibody labeling in dissociated hippocampal cultures (scale bar, 10  $\mu m$ ). Labeling in  $K^+$ -treated cultures was greater than under control conditions. Right: the graph depicts group averages of LAMP-2 labeling ( $n = 10$ –23 cells/condition). NED-19 and bafilomycin prevented activity-dependent increases in LAMP-2 labeling.

Significance was assessed with Kruskal-Wallis and post hoc Dunn's tests. Error bars represent SEM. See also Figure S6 and Movie S1.

These findings suggest that membrane depolarization mobilized lysosomes close to the cell surface and in a manner dependent on lysosomal  $Ca^{2+}$  signaling; however, from these data alone, we could not determine whether such mobilization was followed by fusion of the lysosome with the plasma membrane.

We next used live-cell immunolabeling in dissociated neurons to examine whether lysosomes were capable of fusing with the plasma membrane in an activity-dependent manner. We applied a fluorescently labeled antibody targeting the luminal domain of the lysosome-associated membrane protein LAMP-2 during  $K^+$ -mediated depolarization. Under these conditions, fluorescent labeling of LAMP-2 would require lysosomes to fuse with the plasma membrane (Figure 4C). Using this technique, we found that membrane depolarization resulted in significantly greater amounts of immunofluorescence in the dendrite compared with control conditions (in arbitrary fluorescence units [AFU];  $K^+$ ,  $35 \pm 4$ ; control,  $24 \pm 2$ ;  $n = 23$  cells/condition; post hoc Dunn's test,  $p < 0.05$ ; Figure 4D). Knocking out LAMP-2 using CRISPR/Cas9 abolished all surface labeling, confirming that immunofluorescence was specifically associated with LAMP-2 labeling (Figure S6). Moreover, pre-incubation of cells with either NED-19 or bafilomycin abolished activity-induced increases

in LAMP-2 fluorescence ( $n = 10$  cells; NED-19 versus NED-19 +  $K^+$ , post hoc Dunn's test,  $p = 0.86$ ;  $n = 11$  cells; bafilomycin versus bafilomycin +  $K^+$ , post hoc Dunn's test,  $p = 0.93$ ; Figure 4D). These findings suggest that neuronal depolarization drives lysosomal fusion with the plasma membrane and in a manner dependent on activity-evoked lysosomal  $Ca^{2+}$  release.

To image lysosomal fusion with improved rapidity and sensitivity, we made use of superecliptic pHlourin (SEP), a pH-sensitive GFP that is commonly used as a probe for synaptic vesicle fusion. We tagged SEP to the luminal domain of LAMP-2 (Figure 5A). The fluorescence of LAMP2-SEP, which would be otherwise quenched in the acidic environment of the lysosome, should be detected upon exposure to the pH neutral environment of the extracellular fluid following lysosomal fusion with the plasma membrane. We expressed LAMP2-SEP in dissociated cultures. LAMP2-SEP localized to lysosomes, retained its pH sensitivity, and exhibited maximal fluorescence upon de-acidification of the lysosome with  $NH_4Cl$  (Figure S7). Moreover, upon  $K^+$  stimulation, we observed a large and rapid increase in LAMP2-SEP fluorescence throughout the dendritic arbor ( $68\% \Delta F/F \pm 17\% \Delta F/F$ ;  $n = 5$  cells; versus baseline; Mann-Whitney test,  $p < 0.05$ ; Figures 5B–5D). This was followed



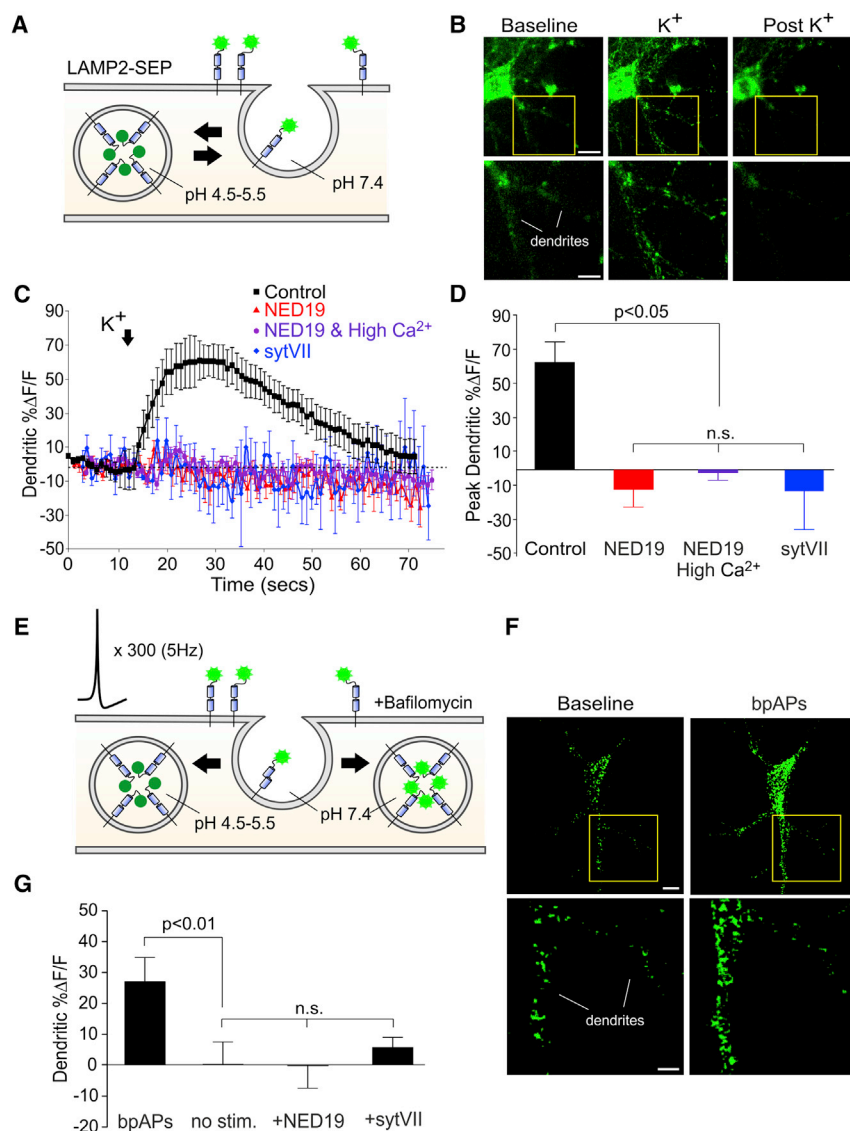


**Figure 5. Imaging Lysosomal Fusion with LAMP2-SEP**

(A) Schematic of LAMP2-SEP. pH-dependent changes in fluorescence were used to monitor lysosomal fusion.

(B) TIRFM image of a dissociated hippocampal neuron transfected with LAMP2-SEP (scale bar, 10  $\mu$ m). The imaged area in the yellow box is magnified below (scale bar, 5  $\mu$ m).

(C and D) Average  $K^+$ -evoked changes in LAMP2-SEP fluorescence in time (D,  $n = 5-7$  cells/condition) with peak changes quantified in (D). Activity-dependent increases in fluorescence were abolished by NED-19 or intracellular loading of Syt7.

(E) Schematic of the experiment using the alkaline trap to examine lysosome fusion in response to bpAPs. Neurons were stimulated with 300 action potentials at 5 Hz in the presence of bafilomycin to prevent re-acidification of the lysosome upon internalization.

(F) Confocal image of a dissociated neuron transfected with LAMP2-SEP (scale bar, 10  $\mu$ m). The imaged area in the yellow box is magnified below (scale bar, 5  $\mu$ m). bpAPs triggered an increase in fluorescence.

(G) Average bpAP-evoked change in LAMP2-SEP fluorescence ( $n = 6-7$  cells/condition). No activity-dependent increases in fluorescence occurred following extracellular application of NED-19 or intracellular loading of Syt7.

Significance was assessed with Kruskal-Wallis and post hoc Dunn's tests. Error bars represent SEM. See also Figure S7 and Movie S2.

by a return to basal fluorescence within 65 s ( $n = 5$  cells; fluorescence at 65 s versus baseline; Mann-Whitney test,  $p = 0.85$ ; Figures 5B and 5C; Movie S2), likely reflecting the surface retrieval and re-acidification of LAMP-2. Fusion of the lysosome with the plasma membrane in several cell types has previously been shown to require the actions of synaptotagmin 7 (Syt7) and can be blocked by loading cells with the cytosolic domain of Syt7 (Martinez et al., 2000; Luzio et al., 2007b). Therefore, to confirm that increases in LAMP2-SEP fluorescence reflected bona fide fusion of the lysosome with the plasma membrane, we loaded cells with the cytosolic domain of recombinant Syt7 (100  $\mu$ g/mL). Under these conditions, we detected no increases in fluorescence following  $K^+$  treatment ( $n = 5$  cells; Syt7 versus control, post hoc Dunn's test,  $p < 0.05$ ; Figures 5C and 5D). Increases in fluorescence were also abolished by NED-19 ( $n = 7$  cells; versus control, post hoc Dunn's test,  $p < 0.05$ ; Figures 5C and 5D), even when  $Ca^{2+}$  influx from VGCCs

from lysosomal stores is integral for the fusion of the lysosome with the plasma membrane even when  $Ca^{2+}$  influx from VGCCs is augmented.

LAMP2-SEP gave us the added advantage of examining whether lysosome fusion could be triggered by dendritic depolarization evoked by bpAPs. Because we could not reliably detect increases in LAMP2-SEP fluorescence to a single bpAP, we made use of the alkaline trap method (Grubb and Burrone, 2009), which blocks vesicle re-acidification with the V-ATPase inhibitor bafilomycin. This would enable fusion-mediated increases in LAMP2-SEP fluorescence, if present, to accumulate to measurable levels during repeated stimulation despite LAMP-2 surface retrieval (Figure 5E). It is important to mention that, although chronic incubation (>60 min) of bafilomycin inhibited lysosomal  $Ca^{2+}$  signaling (Figure 2B), acute applications had no effect, likely because of the poor membrane permeability of the drug. In keeping with this, brief application of bafilomycin

(<10 min) in the absence of any electrical stimulation produced no change in LAMP2-SEP fluorescence ( $n = 6$  cells;  $z$  test versus 0,  $p = 0.93$ ; Figure 5G), suggesting that the drug alone had no effect on lysosomal pH. However, we did observe robust increases in fluorescence when bafilomycin application was followed by low-frequency (5-Hz) stimulation of 300 bpAPs, which was achieved using field electrodes ( $27\% \Delta F/F \pm 6\% \Delta F/F$ ;  $n = 6$  cells; versus no stimulation; post hoc Dunn's test,  $p < 0.01$ ; Figures 5F and 5G). No such increases were observed when stimulation was delivered in the presence of NED-19 ( $n = 7$  cells; versus no stimulation; post hoc Dunn's test,  $p = 0.99$ ; Figure 5G) or following intracellular loading of Syt7 ( $n = 5$  cells; versus no stimulation; post hoc Dunn's test,  $p = 0.44$ ; Figure 5G). Our findings suggest that bpAP-evoked lysosomal  $\text{Ca}^{2+}$  release triggers lysosomal fusion with the plasma membrane.

### Lysosomal Fusion Results in the Release of Cathepsin B

The fusion of the lysosome with the plasma membrane likely results in the release of its contents into the extracellular space. We hypothesized that the release of lysosomal proteases may be required for the activity-dependent restructuring of the extracellular matrix (ECM). This would be of potential relevance for long-term synaptic changes, which are known to require ECM remodelling (Włodarczyk et al., 2011; Dziembowska and Włodarczyk, 2012). In this regard, Cathepsin B was of particular interest to us. The cathepsins are a family of lysosomal proteases that generally show preferential activation in acidic environments. Cathepsin B, however, exhibits enzymatic activity in both acidic and pH-neutral environments, suggesting that, upon lysosomal fusion, Cathepsin B would likely retain some form of enzymatic activity in the pH-neutral extracellular space (Mort et al., 1984; Linebaugh et al., 1999).

We first examined whether Cathepsin B could, in fact, be released by neuronal lysosomes in an activity-dependent manner. We incubated dissociated hippocampal neurons with Magic Red Cathepsin B fluorogenic substrate, which fluoresces upon Cathepsin B-mediated cleavage. Application of the substrate resulted in labeling of fluorescent puncta that co-localized with LysoTracker, confirming that active Cathepsin B was ubiquitously present in neuronal lysosomes (Figure 6A; Figure S8). Magic Red fluorescence also co-localized with Cathepsin B-GFP fluorescence, confirming that it was labeling Cathepsin-B containing compartments (Figure S8). We then stimulated cultures with 45 mM  $\text{K}^+$  and found that this resulted in a loss of Magic Red fluorescence in some of the imaged puncta, consistent with the notion of lysosomal exocytosis, and the loss of Cathepsin B activity from these sites (Figure 6A). A similar loss of fluorescence was seen with LysoTracker (Figure 6A; Figure S8). The average loss of Magic Red fluorescence across puncta ( $-15.6\% \Delta F/F \pm 1.6\% \Delta F/F$ ;  $n = 226$  puncta from 6 cells; Figure 6B) was significantly greater than in unstimulated cultures ( $n = 254$  puncta from 5 cells; post hoc Dunn's test,  $p < 0.01$ ; Figure 6B), and in cultures pre-treated with NED-19 ( $n = 152$  puncta from 5 cells; post hoc Dunn's test,  $p < 0.01$ ; Figure 6B). We defined puncta undergoing fusion as those exhibiting a loss of Magic Red fluorescence of  $>3$  SD from the average fluorescent change measured in unstimulated control experiments. Using this metric, we found that, with  $\text{K}^+$  stimulation, the fraction of

Cathepsin B puncta undergoing fusion ( $8.4\% \pm 1.8\%$ ;  $n = 226$  puncta from 6 cells; Figure 6C) was significantly greater than that found in unstimulated controls ( $n = 254$  puncta from 5 cells; corrected  $z$  test,  $p < 0.01$ ; Figure 6C) or in cultures pre-treated with NED-19 ( $n = 152$  puncta from 5 cells; versus  $\text{K}^+$  stimulation; corrected  $z$  test,  $p < 0.01$ ; Figure 6C). Live-cell immunolabeling of synapses with anti-GluA1 antibodies additionally revealed that  $>95\%$  of Cathepsin B puncta, both the total pool of puncta and those undergoing activity-dependent fusion, were located within  $1 \mu\text{m}$  of a GluA1-labeled punctum (Figure S8), suggesting that Cathepsin B release occurs in the vicinity of synapses.

### Cathepsin B Release Activates MMP-9

ECM remodelling is canonically associated with matrix metalloproteinases (MMPs). One means by which Cathepsin B can promote ECM remodelling is by recruiting MMP activity. It does so by cleaving TIMP-1, an endogenous and potent inhibitor of MMP signaling (Kostoulas et al., 1999; Murphy and Lynch, 2012). We therefore examined whether activity-dependent release of lysosomal Cathepsin B could contribute to ECM remodeling in cultured hippocampal slices. Using an ELISA, we first confirmed whether we could detect activity-dependent elevations of Cathepsin B in the extracellular fluid. Similar to our findings in dissociated neurons, we found that  $\text{K}^+$  treatment elevated extracellular Cathepsin B in hippocampal slices (in a.u.; control,  $0.19 \pm 0.011$ ;  $n = 8$  slices;  $\text{K}^+$ ,  $0.31 \pm 0.006$ ;  $n = 5$  slices; post hoc Bonferroni test,  $p < 0.01$ ; Figure 6D). Pre-treatment with NED-19 greatly reduced this activity-dependent increase ( $n = 7$  slices; NED-19 +  $\text{K}^+$  versus  $\text{K}^+$ ; post hoc Bonferroni test,  $p < 0.01$ ; Figure 6D), although it did not quite abolish it ( $n = 7$  and 5 slices; NED-19 versus NED-19 +  $\text{K}^+$ ; post hoc Bonferroni test,  $p < 0.05$ , Figure 6D). We next examined whether extracellular Cathepsin B was enzymatically active. To do so, we incubated slices with a Cathepsin B fluorogenic substrate (Z-Arg-Arg-AMC) and monitored increases in extracellular fluorescence as a readout of enzymatic activity (Figure 6E). Cathepsin B activity was minimal under control conditions ( $77 \pm 502$  AFU;  $n = 5$  slices;  $z$  test versus 0,  $p = 0.87$ ; Figure 6E), greatly enhanced after  $\text{K}^+$  stimulation ( $1,717 \pm 850$  AFU;  $n = 5$  slices;  $\text{K}^+$  versus control; post hoc Bonferroni test,  $p < 0.05$ ; Figure 6E), and abolished by NED-19 ( $n = 5$  slices/condition; NED-19 versus NED-19 +  $\text{K}^+$ ; post hoc Bonferroni test,  $p = 0.99$ ; Figure 6E). Collectively, these findings are consistent with the activity-dependent release of active Cathepsin B from lysosomal stores.

Cathepsin B is able to activate MMP signaling by cleaving the MMP inhibitor TIMP-1 (Kostoulas et al., 1999; Murphy and Lynch, 2012). We therefore examined whether activity-dependent release of lysosomal Cathepsin B could mediate an increase in extracellular MMP activity in hippocampal tissue. To examine this, we incubated hippocampal slices with a broadly selective MMP fluorogenic substrate (PEPDAB0502), which fluoresces upon MMP-mediated cleavage (Miller et al., 2011). We examined MMP-associated fluorescence either in the presence or absence of the membrane-impermeable Cathepsin B inhibitor CA-074 ( $1 \mu\text{M}$ ), which we used to selectively inhibit extracellular Cathepsin B activity (Linebaugh et al., 1999; Mitrović et al., 2016). Notably, we saw no effect of CA-074 on MMP activity under basal conditions (in AFU; control,  $2,083 \pm 207$ ;  $n = 29$  slices;

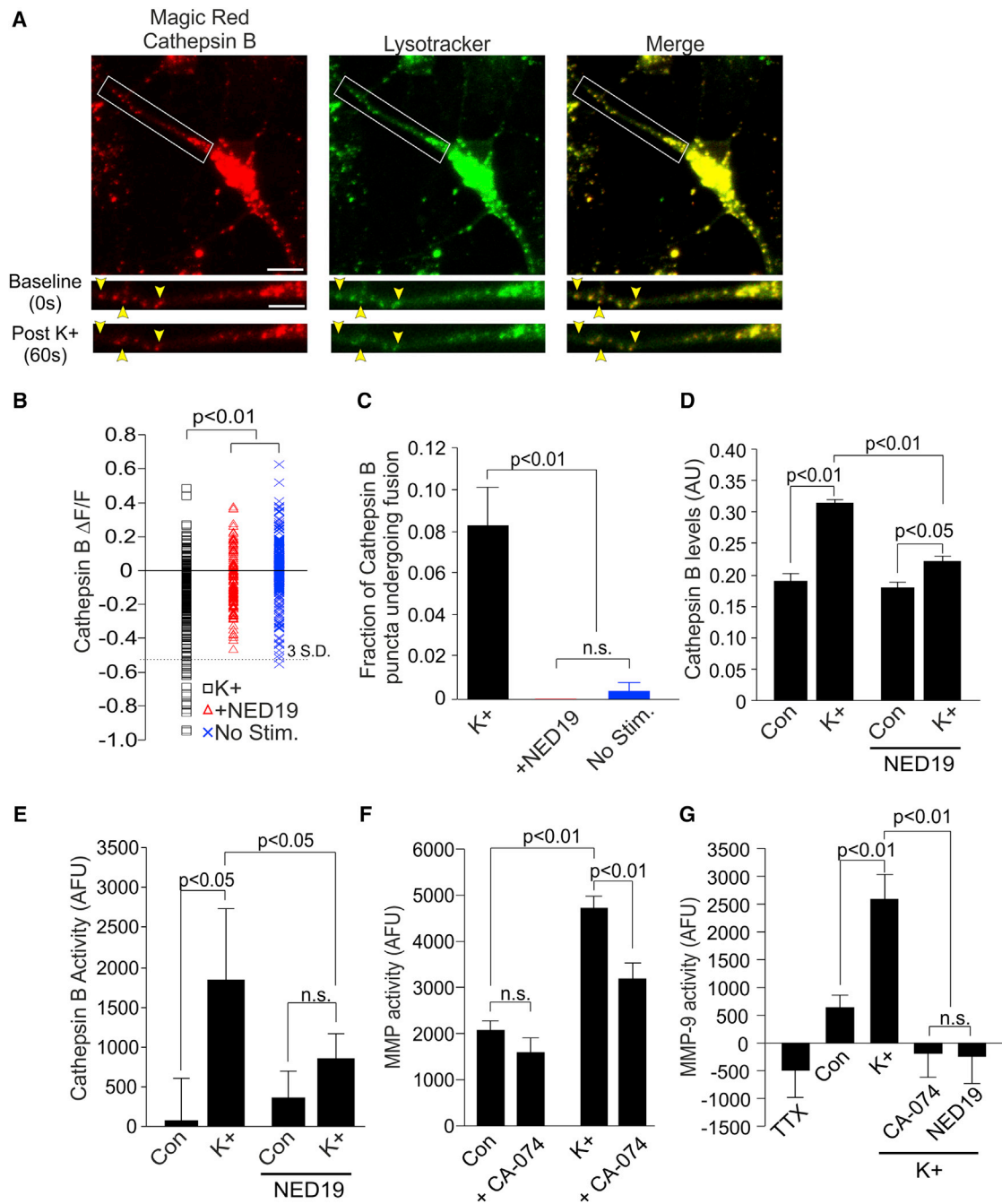


**Figure 6. Lysosomal Fusion Results in the Release of Cathepsin B, which Activates MMP-9 Signaling**

(A) Confocal image of a dissociated hippocampal neuron (scale bar, 10  $\mu$ m) loaded with Magic Red Cathepsin B fluorogenic substrate (red) and LysoTracker (green). The dendrite in the white box is magnified below (scale bar, 5  $\mu$ m). Cathepsin B-associated fluorescence co-localized with LysoTracker-labeled puncta (yellow). Application of 45 mM K<sup>+</sup> resulted in de-staining of some of the imaged puncta (yellow arrowheads), consistent with lysosomal fusion and loss of Cathepsin B activity.

(B) Activity-dependent change in Cathepsin B-associated fluorescence of imaged puncta across experiments ( $n = 152$ –254 puncta from 5–6 cells/condition). The dashed line marks 3 SD from average fluorescent changes recorded in unstimulated controls (no stim.). Significance was assessed with Kruskal-Wallis and post hoc Dunn's tests.

(C) Fraction of Cathepsin B puncta undergoing fusion, as defined by a fluorescence loss of  $>3$  SD (dashed line in B). NED-19 prevented activity-dependent loss of Cathepsin B activity. Significance was assessed with z tests (Bonferroni correction).

(D) Extracellular Cathepsin B expression levels in hippocampal slices measured using ELISA ( $n = 5$ –7 slices/condition). Activity was stimulated by elevating extracellular K<sup>+</sup> to 30 mM. Activity-dependent increases in Cathepsin B secretion were abolished with NED-19.

(legend continued on next page)

CA-074,  $1,601 \pm 317$ ;  $n = 15$  slices; post hoc Bonferroni test,  $p = 0.40$ ; [Figure 6F](#)). However, given our finding that Cathepsin B release is activity-dependent, we repeated the experiment under high  $K^+$  conditions to promote Cathepsin B secretion from lysosomal stores. Under these conditions we found that MMP activity was significantly greater than that of controls (AFU =  $4,725 \pm 259$ ;  $n = 13$  slices;  $K^+$  versus control; post hoc Bonferroni test,  $p < 0.01$ ; [Figure 6F](#)) and now sensitive to Cathepsin B inhibition by CA-074 (AFU =  $3,187 \pm 317$ ;  $n = 12$  slices; CA-074 versus  $K^+$ ; post hoc Bonferroni test,  $p < 0.01$ ; [Figure 6F](#)). These findings are consistent with the idea that activity-dependent release of Cathepsin B stimulates MMP activity in hippocampal slices.

Several studies have demonstrated that MMP-9, in particular, is necessary for the maintenance of long-term potentiation (LTP) and dendritic spine growth ([Wang et al., 2008](#); [Włodarczyk et al., 2011](#); [Dziembowska and Włodarczyk, 2012](#)). We were therefore interested in examining how Cathepsin B affected MMP-9 activity in hippocampal slices. For this purpose, we again incubated slices with the MMP fluorogenic substrate but did so either in the presence or absence of an MMP-9 inhibitor (100 nM MMP-9 inhibitor I). We took the reduction in MMP-associated fluorescence that occurred in the presence of the inhibitor as a readout of the levels of MMP-9 activity present under a particular condition. Under control conditions, we detected a small but significant level of MMP-9 activity (AFU =  $635 \pm 220$ ;  $n = 14$  slices;  $z$  test,  $p < 0.01$ ; [Figure 6G](#)). Given that MMP-9 activation is driven by neuronal activity and not normally detectable under baseline conditions ([Nagy et al., 2006](#); [Dziembowska et al., 2012](#)), we reasoned that the MMP-9 activity in our experiment was likely driven by spontaneous neuronal activity in our slices. Indeed, we found that MMP-9 activity was abolished in the presence of TTX ( $n = 9$  slices;  $z$  test versus 0,  $p > 0.05$ ; [Figure 6G](#)), although this did not reach significance compared with control levels of activity (post hoc Bonferroni test,  $p = 0.21$ ). Conversely, elevating neuronal activity by  $K^+$  stimulation greatly enhanced MMP-9 activity from control levels (AFU =  $2,592 \pm 439$ ;  $n = 10$  slices;  $K^+$  versus control; post hoc Bonferroni test,  $p < 0.01$ ; [Figure 6G](#)). Given that  $K^+$  stimulation also enhances Cathepsin B release, we asked whether activity-dependent release of Cathepsin B was necessary for the activity-dependent increase in MMP-9 activity. We found that addition of either CA-074, to inhibit extracellular Cathepsin B, or NED-19, to prevent activity-dependent Cathepsin B release, abolished MMP-9 activity in  $K^+$  stimulated slices (CA-074,  $n = 11$  slices; versus  $K^+$ ; post hoc Bonferroni test,  $p < 0.01$ ; NED-19,  $n = 5$  slices; post hoc Bonferroni test, versus  $K^+$ ,  $p < 0.01$ ; [Figure 6G](#)). Therefore, activity-dependent increase of MMP-9 activity in hippocampal slices requires activity-dependent release of Cathepsin B.

MMP-9 and its endogenous inhibitor TIMP-1 co-localize to secretory vesicles and are co-released with neuronal activity ([Nagy et al., 2006](#); [Sbai et al., 2008](#); [Dziembowska et al., 2012](#)). MMP-9 activity, therefore, will not necessarily depend on the absolute levels of MMP-9 in tissue but on the ratio of MMP-9 to TIMP-1. Therefore, to provide additional evidence that Cathepsin B is capable of recruiting MMP-9 activity, we examined the MMP-9/TIMP-1 ratio in hippocampal slices. We reasoned that this ratio should be increased by neuronal activity and in a manner dependent on lysosomal Cathepsin B. In agreement with this, western blot analysis showed a marked increase in the MMP-9/TIMP-1 ratio in slices treated with  $K^+$  ([Figure S9](#)). Inhibiting Cathepsin B release with NED-19 or Cathepsin B activity with CA-074 inhibited these increases ([Figure S9](#)).

### Cathepsin B Release Is Necessary for MMP-9-Mediated Long-Lasting Structural Plasticity

Long-lasting changes in synaptic function are thought to ultimately require stable, structural changes in the pre- or post-synaptic elements, with LTP induction being associated with long-lasting expansion of the postsynaptic density and a stable enlargement of the dendritic spine head. Such changes require ECM remodelling by MMP-9 ([Wang et al., 2008](#); [Włodarczyk et al., 2011](#); [Dziembowska and Włodarczyk, 2012](#)). Given that lysosomal-mediated release of Cathepsin B provides a means by which neuronal activity can trigger activation of MMP-9, we hypothesized that the lysosome would play a pivotal role in the maintenance of structural plasticity. We therefore examined the effect that inhibiting lysosomal  $Ca^{2+}$  signaling and fusion with NED-19 would have on structural enlargements of dendritic spines induced by Hebbian pairing. For this purpose, we filled CA1 neurons with Alexa Fluor 488 dye to visualize spine structure and induced LTP by pairing brief (1 ms) photolysis of caged glutamate on a target spine with 3–5 bpAPs ([Figure 7A](#)). The pairing was repeated 60 times at 5 Hz. This protocol produced a rapid and long-lasting expansion of the target spine that was present at 1 min following stimulation (fold $\Delta$  =  $1.75 \pm 0.12$ ;  $n = 9$  cells;  $z$  test versus 1.00,  $p < 0.01$ ; [Figures 7B](#) and [7E](#)) and remained stable for at least 60 min thereafter ( $n = 9$  cells; fold $\Delta$  at 60 min versus 1 min; Mann-Whitney,  $p = 0.61$ ; [Figure 7B](#)). No enlargements were observed at neighboring spines ( $n = 9$  cells;  $z$  test versus 1.00,  $p = 0.37$ ; [Figures 7B](#) and [7E](#)). Remarkably, NED-19 abolished long-lasting changes in structural growth ( $n = 6$  cells; fold $\Delta$  at 60 min;  $z$  test versus 1.00,  $p = 0.78$ ; [Figures 7B](#) and [7E](#)) despite having no effect on the initial spine growth recorded 1 min after paired stimulation ( $n = 6$  cells; versus control; Kruskal-Wallis,  $p = 0.29$ ; [Figures 7B](#) and [7E](#)); similar results were obtained when lysosomal  $Ca^{2+}$  release was instead inhibited with desensitizing concentrations of NAADP in the recording electrode ( $n = 6$  cells; fold $\Delta$  at 1 min versus

(E) Extracellular Cathepsin B activity levels measured in hippocampal slices using the fluorogenic Cathepsin B substrate Z-Arg-Arg-AMC ( $n = 5$  slices/condition). Activity-dependent increases in Cathepsin B activity were abolished by NED-19.

(F) Average MMP activity in hippocampal slices measured using an MMP fluorogenic substrate ( $n = 12$ –29 slices/condition). Cathepsin B inhibition with CA-074 reduced MMP signaling in an activity-dependent manner.

(G) Average MMP-9 fluorogenic activity in hippocampal slices ( $n = 5$ –14 slices/condition; [Experimental Procedures](#)). MMP-9 activity was driven by  $K^+$  stimulation and abolished by NED-19 and CA-074. Significance was assessed with ANOVA and post hoc Bonferroni tests.

Error bars represent SEM. See also [Figures S8](#) and [S9](#).



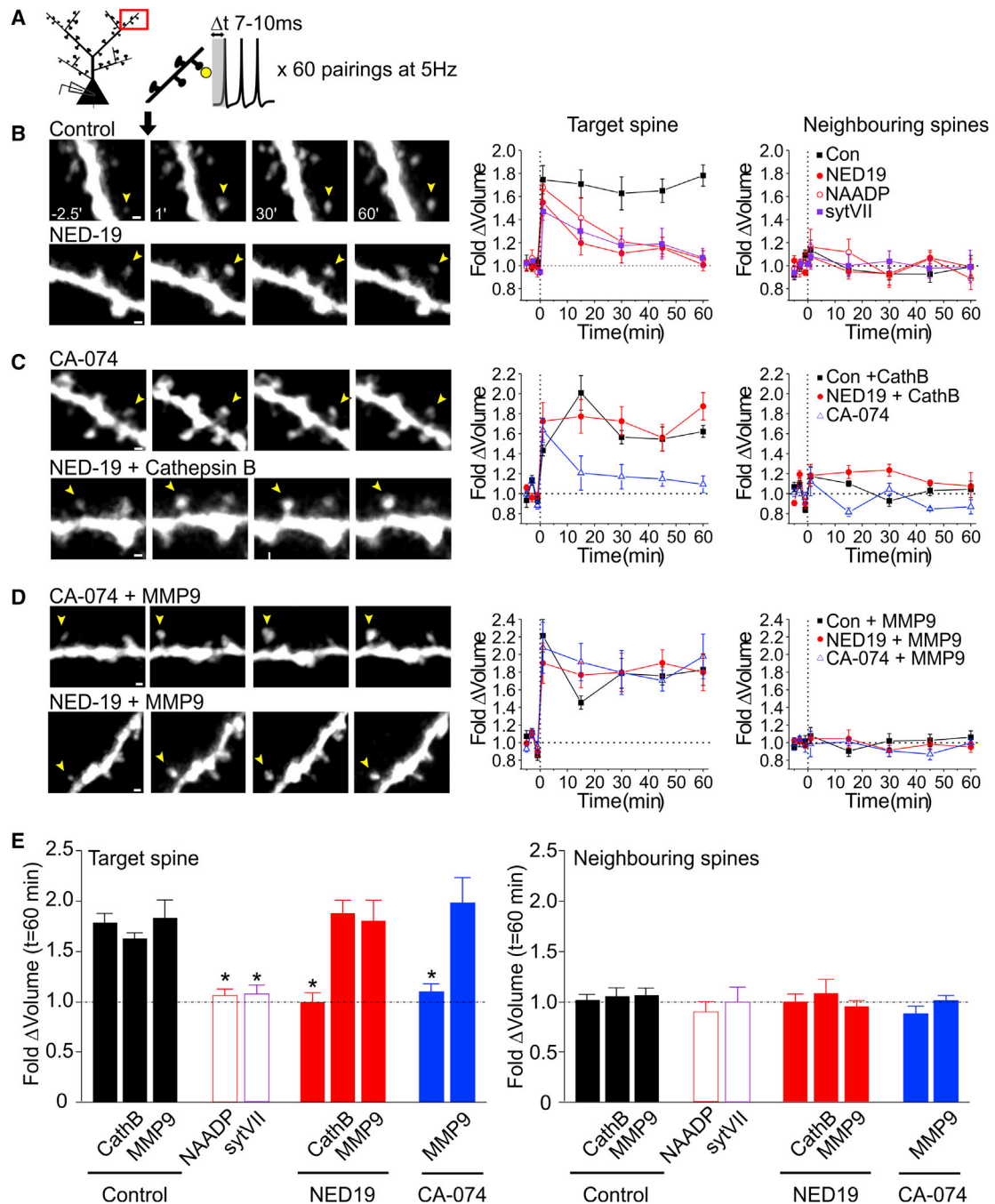


**Figure 7. Cathepsin B Release Is Necessary for MMP-9-Mediated Long-Lasting Structural Plasticity**

(A) Schematic of the experiment. Glutamate photolysis at a target spine was paired with bpAPs to induce long-lasting structural plasticity. (B–D) Left: sample images of CA1 dendritic spines (scale bars, 1  $\mu$ m). Images of target (yellow arrow) and neighboring spines are shown at -2.5, +1, +30, and +60 min following paired stimulation. Right: average change in spine volume of target and neighboring spines across time (n = 5–9 cells/condition). Long-lasting structural plasticity was abolished by inhibiting lysosomal function with NED-19, desensitizing concentrations of NAADP, or intracellular loading of Syt7 (B). Structural plasticity was also abolished by inhibiting Cathepsin B activity with CA-074 (C). Bath application of either active Cathepsin B (C) or active MMP-9 (D) for 10 min after the start of paired stimulation rescued long-lasting structural plasticity. Neighboring spines remained unchanged across experimental conditions. (E) Average change in spine volume at 60 min post-pairing for target and neighboring spines (n = 5–9 cells/condition). Significance was assessed with Kruskal-Wallis and post hoc Dunn's tests. Asterisks denote the significant differences (p < 0.05) from control conditions. All other comparisons with control groups are not significant. Error bars represent SEM.



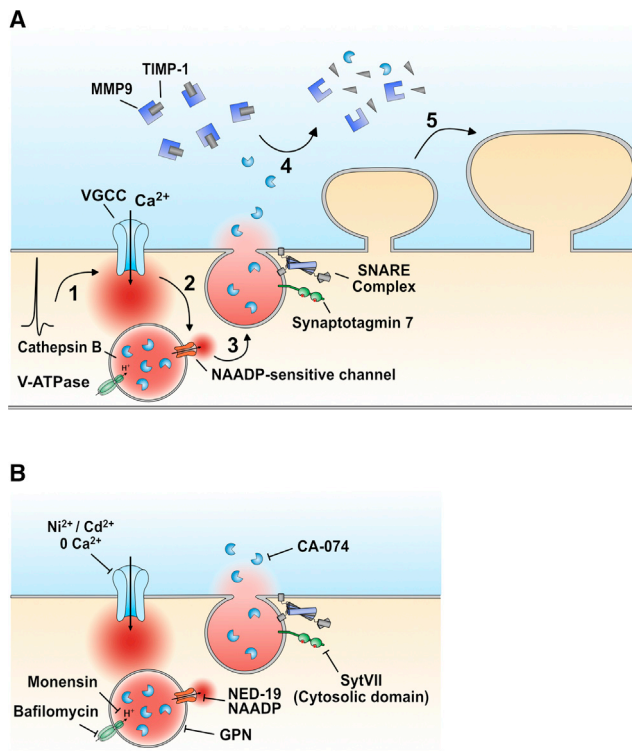


**Figure 8. Proposed Model**

(A) 1: bpAPs activate dendritic VGCCs. 2: VGCC-mediated  $\text{Ca}^{2+}$  influx triggers  $\text{Ca}^{2+}$  release from the lysosome via an NAADP-sensitive channel. 3: lysosomal  $\text{Ca}^{2+}$  release triggers fusion of the lysosome with the plasma membrane, resulting in the release of Cathepsin B. 4: Cathepsin B cleaves TIMP-1, releasing MMP-9 from inhibition. 5: MMP-9 activity maintains the long-lasting structural plasticity of dendritic spines.

(B) Targets of pharmacological reagents used in this study.

control; Kruskal-Wallis,  $p = 0.29$ ; fold $\Delta$  at 60 min,  $z$  test versus 1.00,  $p = 0.46$ ; Figures 7B and 7E) or when lysosomal fusion was inhibited with intracellular loading of the cytosolic domain of Syt7 ( $n = 5$  cells; fold $\Delta$  at 1 min versus control; Kruskal-Wallis,  $p = 0.29$ ; fold $\Delta$  at 60 min;  $z$  test versus 1.00,  $p = 0.46$ ; Figures 7B and 7E). These findings suggest that lysosomal  $\text{Ca}^{2+}$  release and fusion are specifically involved in the maintenance, as opposed to the induction, of structural plasticity; a very similar role has been reported for MMP-9 (Wang et al., 2008). We hypothesized that the reason why pharmacological impairment of lysosomal function prevented structural plasticity was a failure of the postsynaptic neuron to release Cathepsin B during neuronal activity. Consistent with this idea, we found that inhibition of extracellular Cathepsin B with CA-074, was able to phenocopy the effects of NED-19 ( $n = 5$  cells; fold $\Delta$  at 1 min; CA-074 versus NED-19; post hoc Dunn's test,  $p = 0.66$ ; fold $\Delta$  at 60 min; CA-074 versus NED-19; post hoc Dunn's test,  $p = 0.99$ ; Figures 7C and 7E), whereas exogenous application of active Cathepsin B (5  $\mu\text{g}/\text{mL}$  applied for 10 min after the start of pairing) rescued the NED-19 phenotype, restoring persistent expansion of the target spine to control levels (fold $\Delta$  at 60 min =  $1.87 \pm 0.14$ ;  $n = 5$  cells; versus control; post hoc Dunn's test,  $p = 0.99$ ; Figures 7C and 7E) without affecting neighboring spines ( $n = 5$  cells;

Kruskal-Wallis test,  $p = 0.72$ ; Figures 7C and 7E). In contrast, addition of active Cathepsin B in control experiments did not further augment spine expansion ( $n = 5$  cells; versus control; post hoc Dunn's test,  $p = 0.99$ ; Figures 7C and 7E), suggesting that Cathepsin B activity was not a limiting factor under normal conditions of plasticity induction. To then test whether the function of lysosome fusion and Cathepsin B release, in the context of structural plasticity, was to ultimately activate MMP-9, we attempted to rescue the plasticity deficits induced by CA-074 and NED-19 by exogenous application of active MMP-9 (5  $\mu\text{g}/\text{mL}$  applied for 10 min after the start of pairing). We found that MMP-9 did indeed restore persistent expansion of the target spine to control levels in both NED-19- and CA-074-treated slices (NED-19 + MMP-9,  $n = 5$  cells; fold $\Delta$  at 60 min versus control; post hoc Dunn's test,  $p = 0.99$ ; CA-074 + MMP-9,  $n = 5$  cells; fold $\Delta$  at 60 min; versus control; post hoc Dunn's test,  $p = 0.99$ ; Figures 7D and 7E) without affecting neighboring spines (NED-19 + MMP-9,  $n = 5$  cells; Kruskal-Wallis test,  $p = 0.72$ ; CA-074 + MMP-9,  $n = 5$  cells; Kruskal-Wallis test,  $p = 0.72$ ; Figures 7D and 7E). Notably, addition of active MMP-9 in control experiments did not further augment spine expansion ( $n = 5$  cells; fold $\Delta$  at 60 min versus control; post hoc Dunn's test,  $p = 0.99$ ; Figures 7D and 7E), suggesting that the activity of MMP-9, like that of Cathepsin B, was not a limiting factor under normal conditions of plasticity induction.

## DISCUSSION

Here we found that dendritic  $\text{Ca}^{2+}$  influx from VGCCs during bpAPs triggered  $\text{Ca}^{2+}$  release from the lysosome. This  $\text{Ca}^{2+}$  release led to the fusion of the lysosome with the plasma membrane, resulting in the release of Cathepsin B and the subsequent recruitment of MMP-9 activity. We found that activity-dependent enhancement of MMP-9 signaling by Cathepsin B was necessary for the maintenance of the long-lasting dendritic spine growth that accompanies Hebbian pairing of synaptic activity with postsynaptic bpAPs (Figure 8A).

Our finding that bpAPs can trigger  $\text{Ca}^{2+}$  release from the lysosome is unexpected because it has long been thought that bpAP-evoked  $\text{Ca}^{2+}$  influx is mediated exclusively by VGCCs with little or no contribution from intracellular stores. The evidence for this comes from the fact that bpAP-evoked  $\text{Ca}^{2+}$  signals are essentially abolished following VGCC inhibition or removal of extracellular  $\text{Ca}^{2+}$  (Jaffe et al., 1992; Christie et al., 1995; Spruston et al., 1995; Helmchen et al., 1996), whereas inhibition of ER or mitochondrial  $\text{Ca}^{2+}$  signaling is without effect (Markram et al., 1995; Emptage et al., 1999; Kovalchuk et al., 2000). We found similar effects in our own study when blocking VGCC-, ER-, and mitochondrion-mediated  $\text{Ca}^{2+}$  signaling; however, we were also able to unmask a role for lysosomal stores. Notably, we found no evidence of lysosomal  $\text{Ca}^{2+}$  release under conditions in which VGCC-mediated  $\text{Ca}^{2+}$  influx was inhibited, suggesting that lysosomal  $\text{Ca}^{2+}$  release was likely triggered by  $\text{Ca}^{2+}$  influx through VGCCs. Others have demonstrated that  $\text{Ca}^{2+}$  from other sources, such as the ER, can trigger lysosomal  $\text{Ca}^{2+}$  release (Patel et al., 2001; Morgan et al., 2013), potentially by directly activating TPCs (Pitt et al., 2010, 2014); although the exact mechanism remains unclear, it does suggest that TPCs are

regulated both by  $\text{Ca}^{2+}$  and by NAADP. To the best of our knowledge, we are the first to report evidence of a functional coupling between VGCCs and lysosomes, which may potentially be a feature unique to excitable tissue. Certainly, such a coupling is an efficient means of endowing lysosomes with voltage sensitivity, thereby enabling lysosomal  $\text{Ca}^{2+}$  release to be driven by neuronal activity.

Although  $\text{Ca}^{2+}$  release from the lysosomes may serve a number of functions, in this study, we found that it drove the fusion of lysosomes with the plasma membrane. Why  $\text{Ca}^{2+}$  release from the lysosome, as opposed to other sources, is particularly important for its fusion with the plasma membrane is not clear, but a similar mechanism is thought to underlie lysosomal exocytosis in other cell types (Davis et al., 2012; Galione, 2015) and suggests that the lysosomal fusion machinery is sensitive to nano-domain  $\text{Ca}^{2+}$  signaling generated locally by the organelle itself. It is, however, important to note that, from our data alone, we cannot determine whether the lysosomes releasing  $\text{Ca}^{2+}$  in response to bpAPs are those that subsequently undergo fusion with the plasma membrane; it is possible that distinct subpopulations of lysosomes may differentially mediate these functions.

We found that fusion of the lysosome was accompanied by the release of Cathepsin B into the extracellular space. Cathepsin B release has generally been reported in the context of pathological conditions. In neural tissue, excessive levels of extracellular Cathepsin B release have been associated with cell death in traumatic brain injury, brain aneurysm, and several neurologic diseases such as aminotrophic lateral sclerosis (ALS), Alzheimer's disease, Parkinson's disease, and Huntington's disease (Pišlar and Kos, 2014; Hook et al., 2015). Potential mediators of Cathepsin B release under these conditions include reactive astrocytes, microglia, and/or macrophages (Ryan et al., 1995; Linebaugh et al., 1999; Kingham and Pocock, 2001; Gan et al., 2004; Murphy and Lynch, 2012). Although the exact mechanism by which these cells release Cathepsin B is not clear, if it involves lysosomal fusion with the plasma membrane, as reported in this study, then pharmacological inhibition of lysosomal  $\text{Ca}^{2+}$  signaling may provide a novel means for preventing excessive Cathepsin B release under pathological conditions.

We showed that Cathepsin B release was essential for the maintenance of long-term structural plasticity, likely by recruiting MMP-9 activity via cleavage of TIMP-1 (Kostoulas et al., 1999; Murphy and Lynch, 2012). Although several studies have demonstrated a role for MMP-9 in long-term synaptic plasticity, the mechanism by which neuronal activity triggers an increase in MMP-9 activity is not completely understood (Włodarczyk et al., 2011; Dziembowska and Włodarczyk, 2012). In the context of LTP, it is known that neuronal stimulation triggers the transport and translation of MMP-9 mRNA in neuronal dendrites, followed by MMP-9 release into the ECM (Nagy et al., 2006; Dziembowska et al., 2012), where it is converted into its active form, likely via plasmin-mediated cleavage of the MMP-9 pro-domain (Włodarczyk et al., 2011). However, upon secretion, MMP-9 is complexed with its inhibitor TIMP-1 (Sbai et al., 2008), which is capable of inhibiting both active and inactive forms of MMP-9 (Ogata et al., 1995). Inhibition of TIMP-1 signaling, therefore, is likely to be crucial for the maintenance of LTP. Based on our results, we would suggest that the activity-dependent secretion of

Cathepsin B from neuronal lysosomes is one possible means by which TIMP-1 signaling can be inhibited (Figure 8).

Although traditionally viewed as the degradative compartment of the cell, a growing body of evidence suggests that the lysosome functions as a  $\text{Ca}^{2+}$  store that is capable of mediating a diverse array of physiological functions across numerous cell types (Galione et al., 2010, 2015). In this study, we examined the role of lysosomes in neurons. Our findings reveal that lysosomes mediate activity-dependent  $\text{Ca}^{2+}$  signaling in the dendrites and, via the release of Cathepsin B, play an important and unexpected role in the long-term maintenance of structural plasticity.

## EXPERIMENTAL PROCEDURES

### Hippocampal Tissue Preparation

All animal work was carried out in accordance with the Animals (Scientific Procedures) Act, 1986 (UK) and under project and personal licenses approved by the Home Office (UK). Acute coronal hippocampal slices (350–400  $\mu\text{m}$ ) were prepared from male Wistar rats (post-natal day 14 [P14]–P21) and perfused (3 mL/min) with ACSF (120 mM NaCl, 2.5 mM KCl, 2 mM  $\text{CaCl}_2$ , 1 mM  $\text{MgCl}_2$ , 1.2 mM  $\text{NaH}_2\text{PO}_4$ , 26 mM  $\text{NaHCO}_3$ , 11 mM glucose, 0.2 mM ascorbic acid, and 1 mM Trolox; pH = 7.2–7.4; 32°C–34°C; 95%  $\text{O}_2$  and 5%  $\text{CO}_2$ ). Cultured hippocampal slices (350  $\mu\text{m}$ ) were prepared from male Wistar rats (P7). Slices (days in vitro [DIV] 10–15) were perfused (1–2 mL/min) with heated ACSF (32°C–34°C). For dissociated cultures, hippocampal cells from P1 male Wistar rats were plated onto 18-mm coverslips (3–6  $\times 10^4$  cells/coverslip), pre-coated with poly-D-lysine (0.1 mg/mL) and fibronectin (0.05 mg/mL), and imaged on DIV 10–21 in Tyrode's buffer (128 mM NaCl, 5 mM KCl, 1 mM  $\text{MgCl}_2$ , 2 mM  $\text{CaCl}_2$ , 4.2 mM  $\text{NaHCO}_3$ , 20 mM glucose, and 15 mM HEPES; pH = 7.2–7.4; 22°C–24°C). For  $\text{K}^+$  stimulation, 30 or 45 mM NaCl was replaced with KCl. See Supplemental Experimental Procedures for further details.

### $\text{Ca}^{2+}$ Imaging and Electrophysiology

CA3 or CA1 cells in hippocampal slices were recorded using either sharp microelectrodes (70–120 M $\Omega$ ) or high-resistance patch electrodes (16–25 M $\Omega$ ) to minimize intracellular dialysis. For  $\text{Ca}^{2+}$  imaging, sharp microelectrodes contained 0.5–1 mM OGB-1 (Thermo Fisher Scientific) dissolved in 200–400 mM potassium acetate. Patch electrodes contained OGB-1 (0.1–0.2 mM) dissolved in internal solution (135 mM KGlucuronate, 10 mM KCl, 10 mM HEPES, 2 mM  $\text{MgCl}_2$ , 2 mM  $\text{Na}_2\text{ATP}$ , and 0.4 mM  $\text{Na}_3\text{GTP}$ ; pH = 7.2–7.4). Apical dendrites were imaged using confocal laser-scanning microscopy and a 488-nm argon laser. bpAPs were triggered with somatic current injection (1–2 nA, 5–10 ms) and recorded with an AxoclAMP-2B amplifier (Axon Instruments). See Supplemental Experimental Procedures for further details.

### Cathepsin B and MMP Assays

Assays were done on slice culture supernatant using a plate reader. Cathepsin B levels were assessed using a colorimetric human Cathepsin B ELISA kit (ab119684, Abcam) according to the manufacturer's instructions. Cathepsin B and MMP activity was assessed by incubating slices either with the Cathepsin B fluorogenic substrate Z-Arg-Arg-AMC (1:200, JA7740, Merck Millipore) or a MMP fluorogenic substrate (5  $\mu\text{M}$  PEPDAB0502, Biozyme) for 2 hr and examining fluorescence in the supernatant. MMP-9 activity levels were calculated as the difference in MMP fluorescence obtained in the absence and presence of an MMP-9 inhibitor (100 nM of MMP-9 inhibitor I). See Supplemental Experimental Procedures for further details.

### Structural Plasticity and Spine Imaging

CA1 cells in slice cultures were patched (16–25 M $\Omega$ ) with KGlucuronate internal solution containing Alexa Fluor 488 (0.1–0.2 mM, Thermo Fisher Scientific). Small dendritic spines (<1  $\mu\text{m}$ ) were targeted for MNI-glutamate spot photolysis using a 405-nm laser (Photonics). LTP was induced by pairing photolysis (1 ms) with three to five action potentials. Pairing was repeated 60 times at 5 Hz. Fractional changes in fluorescence of the spine head, standardized to

that of the underlying dendrite, were used to estimate fractional changes in spine volume. See [Supplemental Experimental Procedures](#) for further details.

### Statistical Analysis

Significance was assessed using parametric tests (two-tailed paired and unpaired *t* test) or non-parametric tests (two-tailed Mann-Whitney test or two-tailed Wilcoxon matched-pairs test) in which a normal distribution of data could not be confirmed. One-sample *z* tests were used for comparisons against a known value. The Pearson correlation coefficient was used for assessing the significance of linear trends. For multiple comparisons, ANOVA and post hoc Bonferroni's tests (parametric) or the Kruskal-Wallis test with post hoc Dunn's tests (non-parametric) were used. In the text, values are quoted as mean  $\pm$  SEM, and significance is quoted either at the  $p < 0.05$  or  $p < 0.01$  level.

### SUPPLEMENTAL INFORMATION

Supplemental Information includes Supplemental Experimental Procedures, nine figures, and two movies and can be found with this article online at <http://dx.doi.org/10.1016/j.neuron.2016.11.013>.

### AUTHOR CONTRIBUTIONS

Z.P. and N.J.E. designed the experiments. Z.P., L.M., S.J.B., M.R., R.T., A.H., and M.L.H. performed and analyzed the experiments. Z.P. and L.M. wrote the manuscript. Z.P. and N.J.E. revised the manuscript. N.J.E. supervised the project.

### ACKNOWLEDGMENTS

The authors thank Professor Fran Platt and Dr. Sridhar Vasudevan and their respective labs for allowing us access to their plate readers. This work was funded by the MRC (UK) (G0501572) and BBSRC (UK) (BB/5018724/1). Z.P. was funded by a junior research fellowship from Magdalen College, Oxford. M.R. was funded by a scholarship from the Rhodes Trust, and S.J.B. was funded by a scholarship from the British Pharmacological Society.

Received: April 15, 2016

Revised: September 2, 2016

Accepted: October 31, 2016

Published: December 15, 2016

### REFERENCES

- Arantes, R.M., and Andrews, N.W. (2006). A role for synaptotagmin VII-regulated exocytosis of lysosomes in neurite outgrowth from primary sympathetic neurons. *J. Neurosci.* 26, 4630–4637.
- Bak, J., White, P., Timár, G., Missiaen, L., Genazzani, A.A., and Galione, A. (1999). Nicotinic acid adenine dinucleotide phosphate triggers  $\text{Ca}^{2+}$  release from brain microsomes. *Curr. Biol.* 9, 751–754.
- Berg, I., Potter, B.V., Mayr, G.W., and Guse, A.H. (2000). Nicotinic acid adenine dinucleotide phosphate (NAADP $^{+}$ ) is an essential regulator of T-lymphocyte  $\text{Ca}^{2+}$ -signaling. *J. Cell Biol.* 150, 581–588.
- Blott, E.J., and Griffiths, G.M. (2002). Secretory lysosomes. *Nat. Rev. Mol. Cell Biol.* 3, 122–131.
- Brailoiu, E., Patel, S., and Dun, N.J. (2003). Modulation of spontaneous transmitter release from the frog neuromuscular junction by interacting intracellular  $\text{Ca}^{2+}$  stores: critical role for nicotinic acid-adenine dinucleotide phosphate (NAADP). *Biochem. J.* 373, 313–318.
- Brailoiu, E., Hoard, J.L., Filipceanu, C.M., Brailoiu, G.C., Dun, S.L., Patel, S., and Dun, N.J. (2005). Nicotinic acid adenine dinucleotide phosphate potentiates neurite outgrowth. *J. Biol. Chem.* 280, 5646–5650.
- Brailoiu, E., Churamani, D., Pandey, V., Brailoiu, G.C., Tuluc, F., Patel, S., and Dun, N.J. (2006). Messenger-specific role for nicotinic acid adenine dinucleotide phosphate in neuronal differentiation. *J. Biol. Chem.* 281, 15923–15928.
- Brailoiu, G.C., Brailoiu, E., Parkesh, R., Galione, A., Churchill, G.C., Patel, S., and Dun, N.J. (2009). NAADP-mediated channel 'chatter' in neurons of the rat medulla oblongata. *Biochem. J.* 419, 91–97.
- Calcraft, P.J., Ruas, M., Pan, Z., Cheng, X., Arredouani, A., Hao, X., Tang, J., Rietdorf, K., Teboul, L., Chuang, K.T., et al. (2009). NAADP mobilizes calcium from acidic organelles through two-pore channels. *Nature* 459, 596–600.
- Cang, C., Bekele, B., and Ren, D. (2014). The voltage-gated sodium channel TPC1 confers endolysosomal excitability. *Nat. Chem. Biol.* 10, 463–469.
- Chazotte, B. (2011). Labeling lysosomes in live cells with LysoTracker. *Cold Spring Harb. Protoc.* 2011, pdb.prot5571.
- Christie, B.R., Eliot, L.S., Ito, K., Miyakawa, H., and Johnston, D. (1995). Different  $\text{Ca}^{2+}$  channels in soma and dendrites of hippocampal pyramidal neurons mediate spike-induced  $\text{Ca}^{2+}$  influx. *J. Neurophysiol.* 73, 2553–2557.
- Davis, L.C., Morgan, A.J., Chen, J.L., Snead, C.M., Bloor-Young, D., Shenderov, E., Stanton-Humphreys, M.N., Conway, S.J., Churchill, G.C., Parrington, J., et al. (2012). NAADP activates two-pore channels on T cell cyto-lytic granules to stimulate exocytosis and killing. *Curr. Biol.* 22, 2331–2337.
- Dziembowska, M., and Włodarczyk, J. (2012). MMP9: a novel function in synaptic plasticity. *Int. J. Biochem. Cell Biol.* 44, 709–713.
- Dziembowska, M., Milek, J., Janusz, A., Rejmak, E., Romanowska, E., Gorkiewicz, T., Tiron, A., Bramham, C.R., and Kaczmarek, L. (2012). Activity-dependent local translation of matrix metalloproteinase-9. *J. Neurosci.* 32, 14538–14547.
- Emptage, N., Bliss, T.V., and Fine, A. (1999). Single synaptic events evoke NMDA receptor-mediated release of calcium from internal stores in hippocampal dendritic spines. *Neuron* 22, 115–124.
- Erecińska, M., Dagani, F., Nelson, D., Deas, J., and Silver, I.A. (1991). Relations between intracellular ions and energy metabolism: a study with monensin in synaptosomes, neurons, and C6 glioma cells. *J. Neurosci.* 11, 2410–2421.
- Galione, A. (2015). A primer of NAADP-mediated  $\text{Ca}^{2+}$  signalling: From sea urchin eggs to mammalian cells. *Cell Calcium* 58, 27–47.
- Galione, A., Morgan, A.J., Arredouani, A., Davis, L.C., Rietdorf, K., Ruas, M., and Parrington, J. (2010). NAADP as an intracellular messenger regulating lysosomal calcium-release channels. *Biochem. Soc. Trans.* 38, 1424–1431.
- Gan, L., Ye, S., Chu, A., Anton, K., Yi, S., Vincent, V.A., von Schack, D., Chin, D., Murray, J., Lohr, S., et al. (2004). Identification of cathepsin B as a mediator of neuronal death induced by Abeta-activated microglial cells using a functional genomics approach. *J. Biol. Chem.* 279, 5565–5572.
- Grubb, M.S., and Burrone, J. (2009). Using pHluorins to Investigate Synaptic Function (eLS).
- Guse, A.H. (2012). Linking NAADP to ion channel activity: a unifying hypothesis. *Sci. Signal.* 5, pe18.
- Helmchen, F., Imoto, K., and Sakmann, B. (1996).  $\text{Ca}^{2+}$  buffering and action potential-evoked  $\text{Ca}^{2+}$  signaling in dendrites of pyramidal neurons. *Biophys. J.* 70, 1069–1081.
- Hook, G., Jacobsen, J.S., Grabstein, K., Kindy, M., and Hook, V. (2015). Cathepsin B is a New Drug Target for Traumatic Brain Injury Therapeutics: Evidence for E64d as a Promising Lead Drug Candidate. *Front. Neurol.* 6, 178.
- Hui, L., Geiger, N.H., Bloor-Young, D., Churchill, G.C., Geiger, J.D., and Chen, X. (2015). Release of calcium from endolysosomes increases calcium influx through N-type calcium channels: Evidence for acidic store-operated calcium entry in neurons. *Cell Calcium* 58, 617–627.
- Jaffe, D.B., Johnston, D., Lasser-Ross, N., Lisman, J.E., Miyakawa, H., and Ross, W.N. (1992). The spread of  $\text{Na}^{+}$  spikes determines the pattern of dendritic  $\text{Ca}^{2+}$  entry into hippocampal neurons. *Nature* 357, 244–246.
- Kingham, P.J., and Pocock, J.M. (2001). Microglial secreted cathepsin B induces neuronal apoptosis. *J. Neurochem.* 76, 1475–1484.
- Kostoulas, G., Lang, A., Nagase, H., and Baici, A. (1999). Stimulation of angiogenesis through cathepsin B inactivation of the tissue inhibitors of matrix metalloproteinases. *FEBS Lett.* 455, 286–290.



- Kovalchuk, Y., Eilers, J., Lisman, J., and Konnerth, A. (2000). NMDA receptor-mediated subthreshold  $\text{Ca}^{2+}$  signals in spines of hippocampal neurons. *J. Neurosci.* 20, 1791–1799.
- Linebaugh, B.E., Sameni, M., Day, N.A., Sloane, B.F., and Keppler, D. (1999). Exocytosis of active cathepsin B enzyme activity at pH 7.0, inhibition and molecular mass. *Eur. J. Biochem.* 264, 100–109.
- Luzio, J.P., Bright, N.A., and Pryor, P.R. (2007a). The role of calcium and other ions in sorting and delivery in the late endocytic pathway. *Biochem. Soc. Trans.* 35, 1088–1091.
- Luzio, J.P., Pryor, P.R., and Bright, N.A. (2007b). Lysosomes: fusion and function. *Nat. Rev. Mol. Cell Biol.* 8, 622–632.
- Markram, H., Helm, P.J., and Sakmann, B. (1995). Dendritic calcium transients evoked by single back-propagating action potentials in rat neocortical pyramidal neurons. *J. Physiol.* 485, 1–20.
- Martinez, I., Chakrabarti, S., Helleveik, T., Morehead, J., Fowler, K., and Andrews, N.W. (2000). Synaptotagmin VII regulates  $\text{Ca}^{2+}$ -dependent exocytosis of lysosomes in fibroblasts. *J. Cell Biol.* 148, 1141–1149.
- Masgrau, R., Churchill, G.C., Morgan, A.J., Ashcroft, S.J., and Galione, A. (2003). NAADP: a new second messenger for glucose-induced  $\text{Ca}^{2+}$  responses in clonal pancreatic beta cells. *Curr. Biol.* 13, 247–251.
- McGuinness, L., Bardo, S.J., and Emptage, N.J. (2007). The lysosome or lysosome-related organelle may serve as a  $\text{Ca}^{2+}$  store in the boutons of hippocampal pyramidal cells. *Neuropharmacology* 52, 126–135.
- Miller, M.A., Barkal, L., Jeng, K., Herrlich, A., Moss, M., Griffith, L.G., and Lauffenburger, D.A. (2011). Proteolytic Activity Matrix Analysis (PrAMA) for simultaneous determination of multiple protease activities. *Integr. Biol. (Camb.)* 3, 422–438.
- Mitrović, A., Mirković, B., Sosić, I., Gobec, S., and Kos, J. (2016). Inhibition of endopeptidase and exopeptidase activity of cathepsin B impairs extracellular matrix degradation and tumour invasion. *Biol. Chem.* 397, 165–174.
- Morgan, A.J., and Galione, A. (2014). Two-pore channels (TPCs): current controversies. *BioEssays* 36, 173–183.
- Morgan, A.J., Platt, F.M., Lloyd-Evans, E., and Galione, A. (2011). Molecular mechanisms of endolysosomal  $\text{Ca}^{2+}$  signalling in health and disease. *Biochem. J.* 439, 349–374.
- Morgan, A.J., Davis, L.C., Wagner, S.K., Lewis, A.M., Parrington, J., Churchill, G.C., and Galione, A. (2013). Bidirectional  $\text{Ca}^{2+}$  signaling occurs between the endoplasmic reticulum and acidic organelles. *J. Cell Biol.* 200, 789–805.
- Morgan, A.J., Davis, L.C., and Galione, A. (2015a). Imaging approaches to measuring lysosomal calcium. *Methods Cell Biol.* 126, 159–195.
- Morgan, A.J., Davis, L.C., Ruas, M., and Galione, A. (2015b). TPC: the NAADP discovery channel? *Biochem. Soc. Trans.* 43, 384–389.
- Mort, J.S., Recklies, A.D., and Poole, A.R. (1984). Extracellular presence of the lysosomal proteinase cathepsin B in rheumatoid synovium and its activity at neutral pH. *Arthritis Rheum.* 27, 509–515.
- Murphy, N., and Lynch, M.A. (2012). Activation of the  $\text{P2X}_7$  receptor induces migration of glial cells by inducing cathepsin B degradation of tissue inhibitor of metalloproteinase 1. *J. Neurochem.* 123, 761–770.
- Nagy, V., Bozdagi, O., Matynia, A., Balcerzyk, M., Okulski, P., Dzwonek, J., Costa, R.M., Silva, A.J., Kaczmarek, L., and Huntley, G.W. (2006). Matrix metalloproteinase-9 is required for hippocampal late-phase long-term potentiation and memory. *J. Neurosci.* 26, 1923–1934.
- Ogata, Y., Itoh, Y., and Nagase, H. (1995). Steps involved in activation of the pro-matrix metalloproteinase 9 (progelatinase B)-tissue inhibitor of metalloproteinases-1 complex by 4-aminophenylmercuric acetate and proteinases. *J. Biol. Chem.* 270, 18506–18511.
- Pandey, V., Chuang, C.C., Lewis, A.M., Aley, P.K., Brailoiu, E., Dun, N.J., Churchill, G.C., and Patel, S. (2009). Recruitment of NAADP-sensitive acidic  $\text{Ca}^{2+}$  stores by glutamate. *Biochem. J.* 422, 503–512.
- Patel, S., Churchill, G.C., Sharp, T., and Galione, A. (2000). Widespread distribution of binding sites for the novel  $\text{Ca}^{2+}$ -mobilizing messenger, nicotinic acid adenine dinucleotide phosphate, in the brain. *J. Biol. Chem.* 275, 36495–36497.
- Patel, S., Churchill, G.C., and Galione, A. (2001). Coordination of  $\text{Ca}^{2+}$  signaling by NAADP. *Trends Biochem. Sci.* 26, 482–489.
- Penny, C.J., Kilpatrick, B.S., Han, J.M., Sneyd, J., and Patel, S. (2014). A computational model of lysosome-ER  $\text{Ca}^{2+}$  microdomains. *J. Cell Sci.* 127, 2934–2943.
- Pişlar, A., and Kos, J. (2014). Cysteine cathepsins in neurological disorders. *Mol. Neurobiol.* 49, 1017–1030.
- Pitt, S.J., Funnell, T.M., Sitsapesan, M., Venturi, E., Rietdorf, K., Ruas, M., Ganesan, A., Gosain, R., Churchill, G.C., Zhu, M.X., et al. (2010). TPC2 is a novel NAADP-sensitive  $\text{Ca}^{2+}$  release channel, operating as a dual sensor of luminal pH and  $\text{Ca}^{2+}$ . *J. Biol. Chem.* 285, 35039–35046.
- Pitt, S.J., Lam, A.K., Rietdorf, K., Galione, A., and Sitsapesan, R. (2014). Reconstituted human TPC1 is a proton-permeable ion channel and is activated by NAADP or  $\text{Ca}^{2+}$ . *Sci. Signal.* 7, ra46.
- Pryor, P.R., Mullock, B.M., Bright, N.A., Gray, S.R., and Luzio, J.P. (2000). The role of intraorganellar  $\text{Ca}^{2+}$  in late endosome-lysosome heterotypic fusion and in the reformation of lysosomes from hybrid organelles. *J. Cell Biol.* 149, 1053–1062.
- Reddy, A., Caler, E.V., and Andrews, N.W. (2001). Plasma membrane repair is mediated by  $\text{Ca}^{2+}$ -regulated exocytosis of lysosomes. *Cell* 106, 157–169.
- Ryan, R.E., Sloane, B.F., Sameni, M., and Wood, P.L. (1995). Microglial cathepsin B: an immunological examination of cellular and secreted species. *J. Neurochem.* 65, 1035–1045.
- Rybalchenko, V., Ahuja, M., Coblenz, J., Churamani, D., Patel, S., Kiselyov, K., and Muallem, S. (2012). Membrane potential regulates nicotinic acid adenine dinucleotide phosphate (NAADP) dependence of the pH- and  $\text{Ca}^{2+}$ -sensitive organellar two-pore channel TPC1. *J. Biol. Chem.* 287, 20407–20416.
- Sandow, A. (1952). Excitation-contraction coupling in muscular response. *Yale J. Biol. Med.* 25, 176–201.
- Sbai, O., Ferhat, L., Bernard, A., Gueye, Y., Ould-Yahoui, A., Thiollay, S., Charat, E., Charton, G., Tremblay, E., Risso, J.J., et al. (2008). Vesicular trafficking and secretion of matrix metalloproteinases-2, -9 and tissue inhibitor of metalloproteinases-1 in neuronal cells. *Mol. Cell. Neurosci.* 39, 549–568.
- Spruston, N., Schiller, Y., Stuart, G., and Sakmann, B. (1995). Activity-dependent action potential invasion and calcium influx into hippocampal CA1 dendrites. *Science* 268, 297–300.
- Wang, X.B., Bozdagi, O., Nikitczuk, J.S., Zhai, Z.W., Zhou, Q., and Huntley, G.W. (2008). Extracellular proteolysis by matrix metalloproteinase-9 drives dendritic spine enlargement and long-term potentiation coordinately. *Proc. Natl. Acad. Sci. USA* 105, 19520–19525.
- Włodarczyk, J., Mukhina, I., Kaczmarek, L., and Dityatev, A. (2011). Extracellular matrix molecules, their receptors, and secreted proteases in synaptic plasticity. *Dev. Neurobiol.* 71, 1040–1053.
- Wu, G.Y., Deisseroth, K., and Tsien, R.W. (2001a). Activity-dependent CREB phosphorylation: convergence of a fast, sensitive calmodulin kinase pathway and a slow, less sensitive mitogen-activated protein kinase pathway. *Proc. Natl. Acad. Sci. USA* 98, 2808–2813.
- Wu, G.Y., Deisseroth, K., and Tsien, R.W. (2001b). Spaced stimuli stabilize MAPK pathway activation and its effects on dendritic morphology. *Nat. Neurosci.* 4, 151–158.
- Zhang, Z., Chen, G., Zhou, W., Song, A., Xu, T., Luo, Q., Wang, W., Gu, X.S., and Duan, S. (2007). Regulated ATP release from astrocytes through lysosome exocytosis. *Nat. Cell Biol.* 9, 945–953.